Convergence in the temperature response of leaf respiration across biomes and plant functional types

Classification: Biological Sciences, Ecology

Title: Convergence in the temperature response of leaf respiration across biomes and plant functional types

Authors: Mary A. Heskel[1,2], Odhran S. O'Sullivan[1,3], Peter B. Reich[4,5], Mark G. Tjoelker[4], Lasantha K. Weerasinghe[1,6], Aurore Penillard[1], John J.G. Egerton[1], Danielle Creek[1,4], Keith J. Bloomfield[1], Jen Xiang[7], Felipe Sinca[8], Zsofia R. Stangl[9], Alberto Martinez-de la Torre[10], Kevin L. Griffin[11,12], Chris Huntingford[10], Vaughan Hurry[13], Patrick Meir[1,14], Matthew H. Turnbull[15], Owen K. Atkin[1,7]*

Affiliations:

[1]Division of Plant Sciences, Research School of Biology, Building 46, The Australian National University, Canberra, ACT 2601, Australia

[2]The Ecosystems Center, Marine Biological Laboratory, Woods Hole, MA 02543 USA

[3]Animal and Plant Sciences, The University of Sheffield, Sheffield, S10 2TN UK

[4]Hawkesbury Institute for the Environment, University of Western Sydney, Penrith, NSW 2751, Australia

[5]Department of Forest Resources, University of Minnesota, 1530 Cleveland Avenue North, St. Paul, MN 55108, USA

[6]Faculty of Agriculture, University of Peradeniya, Peradeniya, 20400 Sri Lanka

[7]ARC Centre of Excellence in Plant Energy Biology, Research School of Biology, Building 134, The Australian National University, Canberra, ACT 0200, Australia

[8]Department of Global Ecology, Carnegie Institution for Science, 260 Panama Street, Stanford University, CA 94305, USA

[9]Umeå Plant Science Centre, Department of Plant Physiology, Umeå University, SE-901 87 Umeå, Sweden

[10]Centre for Ecology and Hydrology, Wallingford OX10 8BB, UK

[11]Department of Earth and Environment Sciences, Columbia University, Palisades NY, 10964, USA

[12]Department of Ecology, Evolution, and Environmental Biology, Columbia University, New York, 10027, USA

[13]Umeå Plant Science Centre, Department of Forest Genetics and Plant Physiology, Swedish University of Agricultural Sciences, SE-901 83 Umeå, Sweden

[14]School of Geosciences, University of Edinburgh, Edinburgh, UK

[15]Centre for Integrative Ecology, School of Biological Sciences, University of Canterbury, Private Bag 4800, Christchurch, New Zealand

*Correspondence to: Owen.Atkin@anu.edu.au

Keywords: temperature sensitivity (Q_{10}), climate models, carbon exchange

Abstract:

Plant respiration constitutes a massive carbon flux to the atmosphere, and a major control on the evolution of the global carbon cycle. It therefore has the potential to modulate levels of climate change due to the human burning of fossil fuels. Neither current physiological, nor terrestrial biosphere models adequately describe its short-term temperature response, and even minor differences in the shape of the response curve can significantly impact estimates of ecosystem carbon release and/or storage. Given this, it is critical to establish whether there are predictable patterns in the shape of the respiration-temperature response curve, and thus in the intrinsic temperature sensitivity of respiration across the globe. Analyzing measurements in a comprehensive database for 231 species spanning seven biomes, we demonstrate that temperature-dependent increases in leaf respiration do not follow a commonly used exponential function. Instead, we find a decelerating function as leaves warm, reflecting a declining sensitivity to higher temperatures that is remarkably uniform across all biomes and plant functional types. Such convergence in the temperature sensitivity of leaf respiration suggests that there are universally applicable controls on the temperature response of plant energy metabolism, such that a single new function can predict the temperature dependence of leaf respiration for global vegetation. This simple function enables straightforward description of plant respiration in the land surface components of coupled Earth System Models. Our cross-biome analyses shows significant implications for such fluxes in cold climates, generally projecting lower values compared to previous estimates.

Significance:

A major concern for terrestrial-biosphere-models is accounting for the temperature response of leaf respiration at regional/global scales. Most widely adopted models incorrectly assume that respiration increases exponentially with rising temperature, with profound effects for predicted ecosystem carbon-exchange. Based on a large study of 231 species in seven biomes, we instead find that the rise in respiration with temperature can be generalized across biomes and plant types, with temperature-sensitivity declining as leaves warm. This finding points to universally-conserved controls on the temperature-sensitivity of leaf energy metabolism. Accounting for the temperature function markedly lowers simulated respiration rates in cold biomes; this finding has important consequences for estimates of carbon storage in vegetation, predicted concentrations of atmospheric carbon dioxide, and future surface temperatures.

Main text:

Plant respiration provides continuous metabolic support for growth and maintenance of all tissues and contributes ~60 Pg C yr^{-1} to the atmosphere (1, 2), with ~50% of the carbon (C) released by whole-plant respiration from leaves (3). As rates of leaf respiration (*R*) vary substantially with changes in temperature (*T*) (4, 5), even slight increases in ambient *T* can lead to increases in the flux of carbon dioxide (CO_2) from leaves to the atmosphere. This has the potential to create concomitant decreases in net primary productivity, and affect the implications of fossil fuel burning by contributing additionally to atmospheric CO_2 levels due to any imposed surface level global warming. Hence, quantification of the *T* response of leaf *R*, and how this response may vary across diverse ecosystems and plant species, is critical to current estimations and future projections of the global carbon cycle (6-8). Evaluating how leaf *R* relates to *T* in terrestrial plants will clarify fundamental controls on energy metabolism and enable more accurate parameterization, as leaf *R*, in addition to photosynthesis (9, 10), has been identified as a major source of uncertainty in models of the global carbon cycle (8, 11). The response of leaf *R* to *T* differs in both magnitude and mechanism with time scale (5); herein, we address how the fundamental short-term response (minutes to hours) varies among plant species and biomes globally.

The short-term *T*-response of leaf *R* is strongly regulated by the *T*-dependence of the reaction rates of enzymes involved in a variety of respiratory pathways in the cytosol and mitochondria within plant cells (5, 12). Given that these many processes influence the realized rates of leaf *R* across broad ranges in *T*, the *T*-dependence of *R* might be expected to vary widely among contrasting thermal regimes and environments, or among species that differ in metabolic capacity or life span. For example, *R*-*T* relations could vary predictably, according to Plant Functional Types (PFTs, groupings of plant species by life history attributes, growth strategies and/or geographic location), or with variation corresponding with types that differ in rates of net photosynthetic CO_2 uptake and potential growth rates (e.g. fast-growing herbs versus slower-growing trees). A key issue, therefore, is whether the *T*-dependence of leaf *R* has spatially invariant features across the Earth's surface, or instead varies as a consequence of genotypic and

multiple environmental factors. This is critically important, as the global estimation of leaf *R* is a significant uncertainty in Terrestrial Biosphere Models (TBMs) and associated land surface components of Earth System Models (ESMs). The latter quantify the global carbon cycle now and project it into the future (8, 11), including feedbacks as a consequence of anthropogenic emissions of CO_2 on climate.

Although it has been known for over a century that the near-instantaneous increase in plant *R* with rising *T* is non-linear (13, 14), there has been uncertainty whether a single general form for the leaf *R*-*T* relationship applies both phylogenetically and biogeographically (15-17). A widely adopted physiological model framework (18, 19) assumes that *R* exhibits an exponential response to *T,* with *R* roughly doubling with every 10°C rise in *T* (corresponding to a fixed "Q_{10}-type" formulation, with $Q_{10} \approx 2.0$). Yet, it has long been recognized that the Q_{10} is often not constant nor close to 2.0 except over a limited *T* range (14, 20), and this pattern is consistent when also considering ecosystem respiration (21). For this reason, alternative models have been developed, including modified Arrhenius formulations, Universal Temperature Dependence (UTD), and *T*-dependent Q_{10} functions (15-17, 22). All of these models attempt to address the shortcomings of an exponential model that provides a fixed *T*-sensitivity term across a wide range of temperatures. Here, we evaluate a comprehensive set of empirical, thermally high-resolution *T* response curves for multiple taxa and environments. Doing so enables a full assessment of the suitability of these quantitative physiological models in accurately representing the variation in the observed short-term *R*-*T* relationship, and implications of the short-term response in different seasons. We aim to significantly improve how the short-term *R*-*T* response is represented, and recognize this is one element of a complex and dynamic process. As leaf *R* is also impacted by acclimation to sustained changes in growth *T*, future modeling work will determine the effect of a more accurate short-term *T* response applied in concert with recent advances in modeling basal rates of leaf *R* (23) and longer-term (weeks to months) acclimation of *R* to changing growth *T*s (24, 25).

Physiological model representations of leaf respiratory *T* responses vary in complexity and in their ability to account for observed biological patterns, such as decreases in the *T* sensitivity of *R* over increasing *T*s (5, 17) (see Supporting Information for model descriptions

and Figs S1-2). Modification of the *T*-sensitivity of leaf *R* (based on (16)) in TBMs and the associated land surface component of ESMs results in significant alterations to modeled carbon fluxes (8, 26), demonstrating the high sensitivity of the carbon cycle simulations to the *R*-*T* function, and thus the need to improve our understanding and quantification of this relationship. The evidence for apparent complexity in the leaf *R*-*T* response (16, 27) and consequences for carbon cycling indicates both the need for, and, opportunity to improve quantification of the leaf *R*-*T* relationship in globally widespread, but thermally contrasting, biomes. Here, we report on filling that critical knowledge gap.

The goals of our study are three-fold: (1) to quantify the *T*-response of leaf *R* through use of a new and comprehensive set of thermally high-resolution field measurements of leaf *R* across large *T* ranges for each leaf; (2) to assess the shape of *T*-response curves in leaves of species representing diverse environments and PFTs; and, (3) to assess the implications of altered *T*-sensitivity of *R* for simulated carbon fluxes using the land surface component of a leading ESM (28). Using new methods (27) that enabled high-resolution measurement of the *T*-dependence of leaf *R* in leaves, we present results from 673 short-term *T* response curves of 231 species collected *in situ* across 18 sites representing contrasting biomes, geographical locations and PFTs (Table S1). Based on this unprecedented dataset of standardized physiological measurements, we provide new evidence of a global, fundamental *T* response of leaf *R* in terrestrial plants and thus a mathematical model that outperforms alternative representations of how leaf *R* responds to *T*. We also show that in cross-biome analyses, application of this mathematical model significantly alters simulated carbon fluxes, particularly in cold climate ecosystems.

Results

Evaluating Temperature Response Models. Our data of high-resolution measurement of the *T* response of leaf *R* enabled a comparison of commonly applied quantitative physiological models to determine which offered the best fit for replicate response curves across the entire 10-45°C range. A comparison of residuals from model estimates for all individual leaf response curves for five models (exponential fixed-Q_{10}, Arrhenius, 'Lloyd & Taylor', variable-Q_{10}, and second-order

log-polynomial function – see Supporting Information) demonstrates that a second-order log-polynomial model best characterized the *T* response of *R* (Fig. S2a). This selection is made on the basis that the polynomial model had the best projections of leaf-*R* against data from over the entire *T* range, has a straightforward application, and is independent from biological assumptions about activation energies; we applied this approach to all measured response curves that collectively comprise the total mean response (Fig. S2b). Accordingly, to best represent our high-resolution leaf *R* measurements quantitatively, all individual leaf *T* response curve data were natural-log-transformed (*ln*) and to those values, a second-order polynomial model was fitted as:

$$ln\ R = a + bT + cT^2 \quad \text{(Eq. 1)}$$

where *R* is the rate at a given leaf *T* , and *a*, *b*, and *c* are coefficients that provided the fit that minimized residuals.

The application of a polynomial model fit to high-resolution *ln R*-*T* response curves provides a three-parameter description of leaf *R* across the *T* range. The *a* parameter, which indicates *ln R* at 0˚C, determines a reference value offset of the response curve. The *b* parameter - the slope of *ln R* vs. *T* plot at 0°C – and the *c* parameter, which represents any quadratic nonlinearity in *ln R* vs. *T* slope with increasing measuring *T*, are both key to describing the fundamental shape of the short-term *T* response of leaf *R*. To assess the influence of site environment and plant form, we analyzed the variation in values of each model parameter, *a*, *b*, and *c* for diverse biomes and PFTs based on individual leaf sample curves. We calculated this variation for both the entire measured *T* range (10-45˚C), as well as for shorter, discrete segments (*i.e.* 15-25˚C) of the entire measured *T* range, in order to evaluate potential influence of measurement *T* range on these parameters. No difference was found between the parameters calculated from shorter, discrete *T*-ranges and the entire measurement *T*-range, (Tables S2-3, Fig. S3), further justifying the applicability of the polynomial function for this response. Together, mean values of *a*, *b*, and *c* parameters create data-derived equations for leaf *R* that clearly mirror observed mean respiratory responses aggregated for discrete levels of the two corresponding factors (*i.e.* biome or PFT, Fig. 1). This approach can also fully capture the deceleration of rates

150 of *R* observed as *T*s increase (Figs. 1, S1), clearly demonstrating the utility of the polynomial
151 formulation for creating realistic models of leaf *R*.
152
153 **Comparison Among Biomes and Plant Functional Types.** Mean species values for the
154 polynomial model parameters (*a, b,* and *c*) at each site were statistically compared by biome and
155 PFTs using a nested mixed-model approach (Table 1). The curves presented in Figure 1 show
156 that rates of leaf *R* at a common *T* were highest in the coldest biomes (i.e. higher *a* values for
157 tundra and high altitude tropical rainforests). By contrast, low altitude tropical forests, the
158 warmest biome included in this study (Table S1), exhibited the lowest value of parameter *a* and
159 the lowest values of leaf *R* over the measurement ranges of *T* (Fig. 1a,b). Similarly, variation in
160 leaf *R* at a common *T* was found among PFTs (Fig. 1c,d).
161 In strong contrast to large differences across biomes and PFTs in leaf *R* at a common
162 measurement *T*, we found that the rise in *R* with *T* as leaves warm follows a remarkably
163 consistent function, suggesting more universal values of parameters *b* and *c*. Figure 1 illustrates
164 the common shape of the response curve to leaf *T* that is almost invariant across plants, despite
165 representing highly diverse growth environments and functional groups. This low variation
166 across species' means of both *b* and *c* parameters is present when grouped by either biome or
167 PFT (Table 1).
168 Based on our observation of a near-universal shared response shape of leaf *R* to *T*, we
169 determined the parameters for our global polynomial *R*-*T* model (GPM) of Eqn (1). The mean
170 polynomial model parameter values for all species included in our study were: $b = 0.1012$ and c
171 $= -0.0005$, which generate the GPM:
172 $$ln\ R = a + 0.1012T - 0.0005T^2 \qquad \text{(Eq. 2)}$$
173 where *ln R* and *a* are as defined for Eq. 1. This equation is an empirically based mathematical
174 model of the instantaneous *T* response of leaf *R* (Fig. 2a). Average leaf *R* for all study species
175 across the 10-45˚ *T* range (within 1˚C temperature bins; untransformed global mean response in
176 Fig. S2b) – the 'global mean data' – can be effectively summarized by the GPM (Fig. 2a).
177 Values of *a* do, though, vary significantly across PFTs and biomes, shifting the curve of Eqn (2);

thus, the *a* parameter value should be appropriately assigned in the GPM to fit the model's application, using a rate measured at a known *T* or values from our global survey (Table S4).

The input of a known value of leaf *R* (R_{Tref} in the below equation), measured at a *T* (T_{ref} in the below equation) with the universal *b* and *c* response curve parameters can be applied to a derivation of our GPM to predict values of leaf *R* (R_T) at a desired *T*, according to:

$$R_T = R_{T_{ref}} \times e^{[0.1012 \cdot (T - T_{ref}) - 0.0005 \cdot (T^2 - {T_{ref}}^2)]} \quad \text{(Eq. 3)}$$

(where $R_{Tref} = \exp(a + 0.1012T_{ref} - 0.0005T_{ref}^2)$). This equation incorporates the common intrinsic *T*-sensitivity of respiration (i.e. response curve shape) observed from our field measurements, and when combined with measured or assumed rates of *R* at T_{ref}, enables prediction of *R* at various *T*s.

The *T*-sensitivity of the GPM (Fig. 2b), here calculated for illustrative purposes using Q_{10} values, shows decreasing sensitivity of leaf *R* with increases in *T*. Up to 35°C, the decline has similarities to (and a steeper slope than) that reported from more limited data by Tjoelker *et al.*(16). Moreover, our new GPM demonstrates that leaf *R* remains more *T*-sensitive at higher leaf *T*s (e.g. near 45°C) than assessed by Tjoelker *et al.*(16).

Impacts on Simulated Annual Respiration. The consequence of using our GPM in existing global models that exclude acclimation responses to sustained changes in growth *T* is illustrated in Figure 3 which shows annually averaged rates of leaf *R* for our 18 field sites, comparing JULES estimates modeled with a $Q_{10} = 2$ with those from our GPM derivation (Eq. 3).

As a sensitivity study, we replaced the derivation of the GPM (Eq. 3) with the commonly applied fixed Q_{10} formulation, setting Q_{10}=2, and compared the two. The difference between annual rates of leaf *R* calculated using either the derived GPM (Eq. 3) or a fixed Q_{10} equation where Q_{10}=2 had almost no impact on at the warm tropical sites (Fig. 3a,b); similarly, there was no effect of the GPM on seasonal variations in leaf *R* at the tropical sites (Fig. 3c). By contrast, at colder sites, estimates of annual leaf *R* were markedly lower when calculated using the GPM derivation (e.g. 28% lower in Toolik Lake, Alaska and 10 to 20% lower in the temperate sites) compared to the fixed Q_{10} function (Fig. 3b), although recognizing these changes are for generally lower *R* values. At temperate woodland sites with evergreen, long-lived foliage,

replacement of a fixed Q_{10} of 2.0 model with the GPM had its greatest absolute and proportional effect during the cold months of winter, but negligible effect during summer months when leaf *T* values were near 25°C. For sites where winters are characterized by winter freezing (and thus where metabolic activity is minimal), use of the GPM reduced estimates of leaf *R* across the entire growing season (Fig. 3c).

Discussion:

Universality of Temperature Response. Despite the huge diversity in plant growth form and local environment represented in our comprehensive dataset, additionally spanning climatic extremes and plant growth rates, we find remarkable convergence in the functional form of the response of leaf *R* to *T*. Basal rates of *R* vary widely amongst biomes and PFTs (Fig. 1), and are known to be related to differences in growth *T*, site aridity and leaf functional traits (23, 34, 35). That *R* at a given *T* is highest in leaves of arctic tundra plants and lowest in leaves of plants from low elevation tropical forests (Fig. 1a) agrees with the concept that leaf *R* (when measured at a common *T*) is higher in plants grown in colder environments (12), and this pattern can be consistently modeled based on known growth *T*s (23). There is significant variation in the curve offset between PFTs; C_3 herbs exhibit the highest rates of leaf *R* across the 10-45˚C range (Fig. 1c), which is also associated with high rates of leaf *R* at a common leaf nitrogen compared to other PFT groups (23, 34). However, here we show the overall shape of the response curve, and thus intrinsic *T* sensitivity of *R*, does not significantly vary; the only variation is an overall offset of the curve. The consistency in the response of leaf *R* to *T* strongly suggests its universality among C_3 plants and that the *T*-dependencies of underlying enzymatic controls of multiple metabolic pathways are widely conserved, even among the most thermally contrasting biomes on Earth. Further, a global, fundamental *T* response can be described in a simple, empirically driven log-polynomial equation, available for incorporating into the land surface component of ESMs and ready to replace current imperfect representations of the short-term *T* response of leaf *R* . Notably, when implemented in a leading Terrestrial Biosphere Model (28) for different geographical regions, this equation significantly reduces annual rates of leaf-level respiration in

cold-climates. We believe this global short-term leaf *R*-*T* response, when applied in conjunction with data-based models of basal leaf *R* (23) and the acclimation response to longer-term growth *Ts* (24), will have important consequences for predicted rates of ecosystem and global carbon exchange, estimates of future carbon storage in vegetation, predicted concentrations of atmospheric CO_2, and impacts of future surface temperatures.

Utility for Predictive Simulation Models. Our finding of a universal *T*-response provides an opportunity for leaf *R* to be better represented in ecosystem models, TBMs and associated land-surface components of ESMs. It is well-known that the use of a fixed-Q_{10} or Arrhenius activation energy leads to inaccuracies in estimations of respiratory efflux, especially at relatively high and low *T*s (5). In particular, Arrhenius-derived functions may overestimate rates at low *T*s and underestimate the decline in *T*-sensitivity of *R* (22) (Fig. S1a). To date, there has been no consensus or consistent assessment based on comprehensive datasets on how to represent the *T* response of *R* in simulation models (36). Our GPM (Eq. 1) and its parameterization (Eqs. 2, 3) against a massive dataset for *R*, is comprised of only three and two coefficients respectively, and offers a simple, yet robust, approach to calculating the *T* response of *R* in leaves. Importantly, our new GPM demonstrates that leaf *R* remains *T*-sensitive at high leaf *T*s (e.g. near 45°C; seen in our Fig. S1a compared to variable Q_{10} model (12), which will have important consequences for predicted rates of respiratory CO_2 efflux at high *T*s, particularly as extreme heat-wave events are predicted to increase in frequency and duration (2).

Application of the GPM requires knowledge of basal rates of leaf *R*, designated by the *a* parameter (Eq. 2) or measured/assumed rates of *R* at a standard measurement $T=T_{Ref}$ (Eq. 3). In cases where the basal rate of *R* is unknown, we suggest application of specific *a* parameter values representing appropriate PFTs and/or biomes (Table 1) or species (Table S4). Alternatively, rates of leaf *R* at common T_{Ref} (25°C) reported in a recent global compilation (23) can be used. We believe future integration of the recent global leaf *R* dataset (23) with the short-term R-T response model defined by our GPM and climatically variable estimates of longer-term *T* response of *R* through acclimation will result in a vastly improved representation of leaf *R* across scales.

Consequences for Terrestrial C Exchange. Our sensitivity study (Fig. 3) showed that while replacing a fixed Q_{10} of two with the GPM will have little impact on calculated rates of leaf *R* in lowland tropical forests, impacts are significant for temperate, boreal and arctic/alpine ecosystems. In such ecosystems, reliance on a fixed Q_{10} greatly overestimates annual leaf *R*, which in turn will result in underestimates of net primary productivity (NPP), as generally TBMs estimate NPP by subtraction of total canopy leaf *R* from modeled estimates of gross primary productivity (GPP). Though future model implementations that consider the extent to which leaf *R* acclimates to long-term changes in air *T* across the globe (24, 25) will likely further improve how leaf *R* is represented in TBMs, our findings point to lower rates of modeled respiratory CO_2 release - and thus possible higher rates of simulated NPP - at sites further away from the equator, compared to current model scenarios. As replacement of a fixed Q_{10} formulation with our GPM is likely to have profound effects on estimates of global plant *R* and calculations of NPP, its adoption in ESMs will adjust projections of both contemporary and future carbon storage in vegetation. This includes estimates of PFT composition in TBMs that also calculate biome extent through NPP-dependent competition rules. Furthermore, via influence on atmospheric CO_2 levels, the GPM will affect estimates of what constitutes 'permissible' fossil fuel emissions needed to stay below any warming thresholds that society determines as unsafe to cross. This might include the presently much-debated limit of two-degree warming since the pre-industrial era (37, 38).

Finally, a priority for environmental science remains the building and operating of ESMs with robust parameterizations, allowing trustworthy forward projections of carbon cycle evolution and assessment of the influence of fossil fuel burning on that cycle and associated implications for future climate change. Plant respiration, and any adjustment to that in response to global warming, places a strong control on Earth's carbon cycle and may modulate human influence on future atmospheric CO_2 concentrations. The urgency to estimate climate change implies ESMs must be operated routinely, both now and in the future. Computational constraints, combined with limited available data, force a compromise in ESMs where numerical code "lumps" features of terrestrial ecosystems into low numbers of PFTs and relatively general

parameterizations. Our study across a massive dataset of leaf *R* measurements, and subsequent testing and fitting to a model of *T* response, shows a remarkable level of invariance between geographical sites and biomes. This provides great encouragement that, for leaf *R* at least, the generality of ESMs can be viewed as a neutral, or perhaps, positive feature.

Methods

Field Sites and Species

Our 18 field sites (see Table S1) cover extensive variation in climate and species diversity across four continents. The seven biomes represented across these sites are: arctic tundra (Tu), boreal forest (BF), temperate deciduous forest (TeDF), temperate woodland (TeW), temperate rainforest (TeRF), high altitude tropical rainforest (TrRF_hi), and high altitude tropical rainforest (TrRF_lw). At each site, a survey of representative woody tree and shrub (and in the Arctic tundra, herbaceous forb) species were selected for measurement. For comparison, these species were classified into the following broad plant functional groups that represent current classification groups in JULES: broadleaved deciduous temperate (BlDcTmp), broadleaved deciduous tropical (BlDcTrp), broadleaved evergreen temperate (BlEvTmp), broadleaved evergreen tropical (BlEvTrp) C_3 herbaceous (C3H), needle-leaved evergreen (NlEv), and broadleaved evergreen shrubs (SEv). A full list of all 231 species included in this study can be found, grouped by site and biome, in Table S4.

High-Resolution Measurements of the Temperature Response of Leaf Respiration

At each field site, replicate branches of sun-lit leaves were cut from plant species and either re-cut under water or placed in plastic bags containing moistened paper towels to minimize desiccation. Post-sampling, all branches were re-cut again and kept in a water-filled bucket; all measurements occurred on the same day as branch sampling. For individual measurements, whole replicate leaves from these branches, or ~10cm shoot segments for conifers and small-leaved species, were placed in a *T*-controlled, well-mixed cuvette, and allowed to adapt to darkness for 30 minutes. Leaf cuvettes were *T*-controlled via a thermostatically-controlled circulating waterbath (model F32-HL, JULABO Labortechnik GmbH, Seelbach, Germany) as in O'Sullivan *et al.* (27) and Heskel *et al.* (39), or via a Peltier system (3010-GWK1 Gas-Exchange Chamber, Walz, Heinz Walz GmbH, Effeltrich, Germany). O'Sullivan *et al*. (27), used the same approach to measurement of *R*-*T* curves, found no differences between attached and detached

leaves, and to allow for higher replication and species sampling, detached leaves were used for this study.

The exiting air-stream from the cuvette was fed to the 'sample' gas line and infrared gas analyzer of a portable gas exchange system (LI-6400xt, Li-Cor Inc., Lincoln, NE, USA), allowing for instantaneous, continuous rates of CO_2 efflux from the darkened leaves across the measurement *T* range. Rates of net exchange were calculated by comparing the 'sample', cuvette-based rates to those of the 'reference' gas line. [CO_2] (set to the prevailing ambient concentration) and flow rate (700 μmol s^{-1}) of the air entering the cuvette chamber were controlled by the LI-6400XT console flow meter and 6400-01 CO_2 mixer. Prior to entering the cuvette chamber, air was routed through the LI-6400XT desiccant column to control relative humidity inside the chamber.

After the 30-minute dark adaption period, the cuvette chamber was cooled to 10°C. Thereafter, the cuvette chamber was heated continuously at a rate of 1°C min^{-1} until a maximum rate of respiration was reached (generally leaf *T* between 55-70°C), although only data up to *T*= 45°C was used in our model. Throughout the warming period, leaf *T* was continuously measured with a small-gauge wire chromel-constantan thermocouple pressed to the lower leaf surface in the cuvette chamber and attached to a LI-6400 external thermocouple adaptor (LI6400-13, Li-Cor Inc., Lincoln, NE, USA), allowing for leaf *T* to be recorded by the LI-6400XT portable gas exchange system. Over the 10-45°C range, leaves typically heated at a rate of 1°C min^{-1} (i.e. matching the rate at which air *T* increased); however, at higher leaf *T*, the rate at which leaf *T* increased often slowed, reflecting an increase in evaporative loss of water from leaf surfaces. The net release of CO_2 from leaves, as determined from the instantaneous difference between 'sample' and 'reference' lines, was recorded at 30s intervals, allowing for ~ two measurements of *R* per 1°C increase in *T*, resulting in a continuous, high-resolution *T* response of *R*.

Post-measurement, each replicate leaf was removed from the cuvette, placed in a drying oven at ~60°C for a minimum of two days, and weighed afterward, so that rates could be expressed on a dry-mass basis (nmol CO_2 g^{-1} s^{-1}). Because the measured replicate leaf often became highly desiccated to accurately measure leaf area, to determine area-based fluxes (μmol CO_2 m^{-2} s^{-1}), a leaf of similar size and shape and adjacent to the measured leaf was digitally

scanned (or determined with a leaf area meter, LI-3100 LiCor Inc., Lincoln, NE, USA), dried, and weighed. The resulting leaf mass per unit area (LMA) of this adjacent leaf could then be used to calculate the area of the measured leaf (assuming a similar LMA) and the area-based *R* fluxes.

Quantification of *R-T* curves and Model Comparison. The 673 *R-T* curves collected by the methods described above required thorough quantification for comparison across replicates, species, sites, biomes, and plant functional types. For each replicate *R-T* response curves, we assessed the fits commonly applied *R-T* models, including: (a) an exponential model with a fixed-Q_{10} across the entire *T* range (though not specifically a fixed Q_{10} of 2, as is applied in some biosphere models of *R*); (b) an Arrhenius model; (c) a model of *R* responding to the UTD as defined by Gillooly *et al*. (15), which contains an activation energy parameter and utilizes Boltzmann's constant; (d) a model presented by Lloyd & Taylor (17) to describe the response of soil *R* to *T* that includes a temperature-sensitive activation energy; (e) a model that incorporates a variable-Q_{10} response across the *T* range as described by two parameters; and (f) a simple second order polynomial model. Equations for these models are shown in Supporting Information. To compare how these models fit to data, we fitted each of the aforementioned models to all replicate *R-T* response curves in JMP (Version 11, SAS Institute, Cary, NC USA), with parameters calculation controlled by the minimal residuals produced from each individual fit for each model. In cases where model convergence was not possible via the curve-fitting software, those replicate curves were not included to calculate mean residuals for the model fit over all replicates. Further, to evaluate the impact of different measurement temperature span (i.e. 10-45˚C vs. 20-45˚C) on model fits, we compared fit coefficients across all replicate curves at different 'segmented intervals' of the response curve (see Table S2, Fig. S3, and Supporting Information text). Using these data, we also compared model fit coefficients from the approximate 20˚C *T*-range that best represents the climate of that species (the "ecologically relevant" *T*-range, see Table S3 and Supporting Information text) to the fit coefficients calculated from all available data from the entire measurement *T*-range.

Global polynomial model (GPM) calculation. After polynomial curve fit analysis, each replicate curve could be defined by specific *a, b,* and *c* parameters. The mean value of replicates

for individual species at given sites were calculated for *a, b,* and *c*, resulting in a total of 231 species-site means of these parameters used for our study. To create a 'global model' of the *T* response of *R*, we calculated the mean of all 231 species-site mean values of the *a*, *b*, and *c* parameters.

Modeling site-based leaf *R* with JULES. For our 18 field sites, we incorporated our derived global *T*-response (Eq. 3), with local values of R_{Tref}, into an offline version of JULES (Joint UK Land Environmental Simulator) to investigate the potential impacts of altered *T*-sensitivity of *R*. JULES is the land surface model of the UK Hadley Centre HadGEM family of Global Circulation Models (28, 40). In its current form, JULES assumes that leaf *R* doubles for every 10°C rise in *T* (i.e. $Q_{10} = 2$); other TBM frameworks have also assumed fixed Q_{10} [e.g. BIOME-BGC (29), PnET-CN (30) CLM4 (31), TEM (32)], or modified Q_{10} [e.g. BETHY (33)] functions. This is done using both the fixed Q_{10} and GPM formulations, and with JULES adopting the site-mean values leaf *R* at $R_{Tref} = 25^{o}C$ derived from our short-term *T*-response curves. The Q_{10} value is set as 2.0 for all 18 sites, and similarly for the GPM model, the *b* and *c* parameters are invariant, taking their cross-site means (Table 1 and Eq. 3).

Here we use a version of JULES driven with the WATCH Forcing Data ERA-interim (WFDEI) surface climatology (41) for each of the 18 sites and for the period 2010-2014 inclusive. Each site uses the WFDEI gridded data values from its 0.5° x 0.5° grid resolution nearest to site location; and in time is therefore a subset of the WFDEI data, presently covering 1979-2014. The DGVM component of JULES is kept switched off, and therefore known local values of LAI are prescribed. Four JULES Plant Functional Types (PFTs) were adopted (Broadleaf Trees, Needleleaf Trees, Shrubs and C_3 grasses/herbs). With the DGVM off, then the main difference between these PFTs is the inclusion of deciduous phenology (where observed, affecting the prescribed LAI), and slightly different response curves for stomatal opening.

Our runs are made for each site, weighed by known fractional covers of the four PFTs above (predominantly broadleaf trees). The actual JULES model diagnostic presented (Fig. 3) is the canopy-top level *R* value (μmol CO_2 $[m^{-2}$ of leaf cover$]^{-1}$ s^{-1}), representing those fluxes that might be observed in fully sun-exposed leaves at the canopy crown, if fluxes from lower leaves were ignored.

Acknowledgements: This work was funded the Australian Research Council grants/fellowships (DP0986823, DP130101252, CE140100008, FT0991448, NERC NE/F002149/1) to OKA, FT110100457 and NERC NE/F002149/1 to PM, DP140103415 to MGT and USA National Science Foundation International Polar Year Grant to KLG. AM and CH acknowledge the CEH National Capability fund.

Author contributions: OKA, MAH, and OSO'S conceived the project with input from MGT. MAH led data compilation, analysis and writing, supported by OKA, OSO'S, PBR and MGT. All authors contributed to data acquisition, writing, intellectual development and/or performed numerical simulations.

Author information: The authors declare no competing financial interests. Readers are welcome to comment on the online version of the paper. Correspondence and requests for materials should be addressed to OKA (Owen.Atkin@anu.edu.au).

References

1. Canadell JG*, et al.* (2007) Contributions to accelerating atmospheric CO_2 growth from economic activity, carbon intensity, and efficiency of natural sinks. *Proc Nat Acad Sci USA* 104:18866-18870.
2. IPCC (2013) Climate Change 2013: The Physical Science Basis. (Cambridge, UK and New York, USA).
3. Atkin OK, Scheurwater I, Pons TL (2007) Respiration as a percentage of daily photosynthesis in whole plants is homeostatic at moderate, but not high, growth temperatures. *New Phytol* 174:367-380.
4. Amthor JS (2000) The McCree-de Wit-Penning de Vries-Thornley Respiration Paradigms: 30 Years Later. *Annals Bot* 86(1):1-20.
5. Atkin OK, Tjoelker MG (2003) Thermal acclimation and the dynamic response of plant respiration to temperature. *Trends Plant Sci* 8(7):343-351.
6. King AW, Gunderson CA, Post WM, Weston DJ, Wullschleger SD (2006) Plant respiration in a warmer world. *Science* 312(5773):536-537.
7. Valentini R*, et al.* (2000) Respiration as the main determinant of carbon balance in European forests. *Nature* 404(6780):861-865.
8. Huntingford C*, et al.* (2013) Simulated resilience of tropical rainforests to CO_2-induced climate change. *Nature Geosci* 6(4):268-273.
9. Pappas C, Fatichi S, Leuzinger S, Wolf A, Burlando P (2013) Sensitivity analysis of a process-based ecosystem model: Pinpointing parameterization and structural issues. *J Geophys Res: Biogeosci* 118(2):505-528.
10. Booth BBB*, et al.* (2012) High sensitivity of future global warming to land carbon cycle processes. *Environ Res Lett* 7(2):024002.
11. Atkin OK, Meir P, Turnbull MH (2014) Improving representation of leaf respiration in large-scale predictive climate–vegetation models. *New Phytol* 202(3):743-748.
12. Atkin OK, Bruhn D, Tjoelker MG (2005) Response of Plant Respiration to Changes in Temperature: Mechanisms and Consequences of Variations in Q_{10}; Values and Acclimation. *Plant Respiration,* Advances in Photosynthesis and Respiration, eds Lambers H & Ribas-Carbo M (Springer Netherlands), Vol 18, pp 95-135.
13. Blackman FF, Matthaei GL (1905) Experimental researches in vegetable assimilation and respiration. IV. A quantitative study of carbon-dioxide assimilation and leaf-temperature in natural illumination. *Proc Roy Soc Lond. Series B*76(511):402-460.
14. Wager HG (1941) On the respiration and carbon assimilation rates of some arctic plants as related to temperature. *New Phytol* 40(1):1-19.
15. Gillooly JF, Brown JH, West GB, Savage VM, Charnov EL (2001) Effects of size and temperature on metabolic rate. *Science* 293(5538):2248-2251.
16. Tjoelker MG, Oleksyn J, Reich PB (2001) Modelling respiration of vegetation: evidence for a general temperature-dependent Q_{10}. *Glob Change Biol* 7(2):223-230.
17. Lloyd J, Taylor JA (1994) On the temperature dependence of soil respiration. *Funct Ecol* 8:315-323.
18. Amthor JS (1984) The role of maintenance respiration in plant growth. *Plant Cell Environ* 7(8):561-569.
19. Ryan MG (1991) Effects of climate change on plant respiration. *Ecol Appl* 1(2):157-167.
20. James WO (1953) *Plant Respiration* (Clarendon Press, Oxford).

21. Mahecha MD, *et al.* (2010) Global convergence in the temperature sensitivity of respiration at ecosystem level. *Science* 329(5993):838-840.
22. Zaragoza-Castells J, *et al.* (2008) Climate-dependent variations in leaf respiration in a dry-land, low productivity Mediterranean forest: the importance of acclimation in both high-light and shaded habitats. *Funct Ecol* 22(1):172-184.
23. Atkin OK, *et al.* (2015) Global variability in leaf respiration in relation to climate, plant functional types and leaf traits. *New Phytol* 206(2):614-636.
24. Vanderwel MC, *et al.* (2015) Global convergence in leaf respiration from estimates of thermal acclimation across time and space. *New Phytol* 207(4):1026-1037.
25. Slot M, Kitajima K (2015) General patterns of acclimation of leaf respiration to elevated temperatures across biomes and plant types. *Oecol* 177:885-900.
26. Wythers KR, Reich PB, Bradford JB (2013) Incorporating temperature-sensitive Q_{10} and foliar respiration acclimation algorithms modifies modeled ecosystem responses to global change. *J Geophys Res: Biogeosci* 118(1):77-90.
27. O'Sullivan OS, *et al.* (2013) High-resolution temperature responses of leaf respiration in snow gum (*Eucalyptus pauciflora*) reveal high-temperature limits to respiratory function. *Plant Cell Environ* 36(7):1268-1284.
28. Clark DB, *et al.* (2011) The Joint UK Land Environment Simulator (JULES), model description - Part 2: Carbon fluxes and vegetation dynamics. *Geosci Model Dev* 4(3):701-722.
29. Wang W, *et al.* (2009) A hierarchical analysis of terrestrial ecosystem model Biome-BGC: Equilibrium analysis and model calibration. *Ecol Mod* 220:2009-2023.
30. Ollinger SV, Aber JD, Reich PB, Freuder RJ (2002) Interactive effects of nitrogen deposition, tropospheric ozone, elevated CO_2 and land use history on the carbon dynamics of northern hardwood forests. *Glob Change Biol* 8(6):545-562.
31. Bonan GB, *et al.* (2011) Improving canopy processes in the Community Land Model version 4 (CLM4) using global flux fields empirically inferred from FLUXNET data. *J Geophys Res: Biogeosci* 116(G2):G02014.
32. Melillo JM, *et al.* (1993) Global climate change and terrestrial net primary production. *Nature* 363(6426):234-240.
33. Ziehn T, Kattge J, Knorr W, & Scholze M (2011) Improving the predictability of global CO_2 assimilation rates under climate change. *Geophys Res Lett* 38(10):L10404.
34. Reich PB, *et al.* (2008) Scaling of respiration to nitrogen in leaves, stems and roots of higher land plants. *Ecol Lett* 11(8):793-801.
35. Reich PB, *et al.* (1998) Relationships of leaf dark respiration to leaf nitrogen, specific leaf area and leaf life-span: a test across biomes and functional groups. *Oecol* 114(4):471-482.
36. Smith NG, Dukes JS (2013) Plant respiration and photosynthesis in global-scale models: incorporating acclimation to temperature and CO_2. *Glob Change Biol* 19(1):45-63.
37. Huntingford C, *et al.* (2012) The link between a global 2 °C warming threshold and emissions in years 2020, 2050 and beyond. *Environ Res Lett* 7: 014039.
38. Rogelj J, *et al.* (2011) Emission pathways consistent with a 2˚C global temperature limit. *Nature Clim Change* 1(8):413-418.
39. Heskel MA, *et al.* (2014) Thermal acclimation of shoot respiration in an Arctic woody plant species subjected to 22 years of warming and altered nutrient supply. *Global Change Biol* 20(8):2618-2630.

40. Best MJ, *et al.* (2011) The Joint UK Land Environment Simulator (JULES), model description - Part 1: Energy and water fluxes. *Geosci Model Dev* 4(3):677-699.
41. Weedon GP, *et al.* (2014) The WFDEI meteorological forcing data set: WATCH Forcing Data methodology applied to ERA-Interim reanalysis data. *Water Resources Res* 50(9):7505-7514.
42. Cox PM, Betts RA, Jones CD, Spall SA, Totterdell IJ (2000) Acceleration of global warming due to carbon-cycle feedbacks in a coupled climate model. *Nature* 408(6809):184-187.
43. Cox P (2001) Description of the "TRIFFID" Dynamic Global Vegetation Model. (Hadley Centre, Met Office, Bracknell, Berkshire), pp 1-16.
44. Poorter H, Remkes C, Lambers H (1990) Carbon and nitrogen economy of 24 wild species differing in relative growth rate. *Plant Physiol* 94(2):621-627.
45. Atkin OK, Scheurwater I, & Pons TL (2007) Respiration as a percentage of daily photosynthesis in whole plants is homeostatic at moderate, but not high, growth temperatures. *New Phytol* 174(2):367-380.
46. Kruse J, Rennenberg H, & Adams MA (2011) Steps towards a mechanistic understanding of respiratory temperature responses. *New Phytol* 189(3):659-677.
47. Elias M, Wieczorek G, Rosenne S, & Tawfik DS (2014) The universality of enzymatic rate-temperature dependency. *Trends Biochem Sci* 39(1):1-7.
48. Hoefnagel MHN, Atkin OK, Wiskich JT (1998) Interdependence between chloroplasts and mitochondria in the light and the dark *Biochim Biophys Acta. Bioenerg* 1366(3):235-255.
49. Wiskich JT, Dry IB (1985) The tricarboxylic acid cycle in plant mitochondria: its operation and regulation. *Encyclopedia of Plant Physiology. Higher Plant Cell Respiration*, eds Douce R & Day DA (Springer Verlag), pp 281-313.
50. Way D, Yamori W (2014) Thermal acclimation of photosynthesis: on the importance of adjusting our definitions and accounting for thermal acclimation of respiration. *Photosyn Res* 119(1-2):89-100.
51. Slot M, Zaragoza-Castells J, Atkin OK (2008) Transient shade and drought have divergent impacts on the temperature sensitivity of dark respiration in leaves of *Geum urbanum*. *Funct Plant Biol* 35(11):1135-1146.
52. Armstrong AF, *et al.* (2008) Dynamic changes in the mitochondrial electron transport chain underpinning cold acclimation of leaf respiration. *Plant Cell Environ* 31(8):1156-1169.
53. Huntingford C, Cox PM, Lenton TM (2000) Contrasting responses of a simple terrestrial ecosystem model to global change. *Ecol Mod* 134(2000):41-58.
54. Monteith JL (1981) Evaporation and surface temperature. *Quart J Royal Meteorol Soc* 107(451):1-27.
55. Hijmans RJ, Cameron SE, Parra JL, Jones PG, Jarvis A (2005) Very high resolution interpolated climate surfaces for global land areas. *Intern J Climat* 25:1965-1978.

564 **Figure Legends**
565
566 **Figure 1.** Mean measured leaf respiration (natural log transformed; ± SE) of biome (**a**) and plant
567 functional types (PFTs) (**c**) calculated for each ˚C from measured species respiration response
568 curves of those categories, for the available temperature ranges. Polynomial models based on
569 species' mean values of *a*, *b*, and *c* (see Table 1) of those biomes (**b**) and PFTs (**d**) are shown
570 across the same *T* range.
571
572 **Figure 2.** Global mean data reflected by modeled *R*-*T* and corresponding declining Q_{10}
573 responses. The mean *T* response of (**a**) natural log transformed rates of leaf respiration (ln *R* +/-
574 SE, "Global Mean Data", shown with blue symbols with error bars) for all measured species (*n* =
575 231) across all biomes and PFTs, overlaid on the Global Polynomial Model (GPM) of ln *R* (solid
576 black line, bracketed by dashed lines representing 95% confidence intervals), calculated from the
577 species values of *a, b*, and *c* parameters of the polynomial model. The GPM is defined as ln *R* = -
578 2.2276 + 0.1012* *T* - 0.0005**T*^{2}. The *T*-response of Q_{10} values (**b**) based on GPM *b* and *c*
579 coefficients as calculated by $Q_{10} = e^{10*(0.1012+(2*0.0005T))}$, shown with 95% confidence intervals
580 (dashed lines).
581
582 **Figure 3.** Impact of two *T*-functions on annual average of modeled instantaneous leaf respiration
583 rates (*R*) using the JULES coupled climate-carbon model to extrapolate respiration
584 measurements (42, 43)**.** Panel (a) shows annual average of leaf *R* (averaged over the five years of
585 2010-2014 inclusive) at 18 globally-distributed field sites (Table S1), with annual rates of *R*
586 calculated assuming a fixed Q_{10} of 2.0 (43) or our Global Polynomial Model (GPM; Eq. 3).
587 Annual averages of leaf *T* (same period) in the upper canopy is shown as green dots. Sites are
588 ordered by temperature, with site codes as shown in Table S1; (b) shows percentage changes in
589 annual averages of rates of leaf *R* that result from switching from a fixed Q_{10} to our GPM,
590 plotted against annual averages of leaf *T* – the dashed line shows a parabolic curve fit i.e. with
591 three degrees of freedom; (c) shows seasonal variation in rates leaf *R* (expressed on a leaf area
592 index (LAI) basis) for three thermally contrasting sites (Toolik Lake (tundra), Alaska; Great
593 Western Woodlands (temperate woodland), Western Australia; and, Paracou (tropical rainforest),
594 French Guiana). Site-averaged leaf *R* values at 25°C, measured in the field, were used for the
595 calculations.
596
597
598
599
600
601
602

Table 1. Biome and plant functional type (PFT) mean values (with 95% confidence intervals) of *a*, *b* and *c* coefficients aggregated across all species (*n* = 231).

Biome	***a***		***b***		***c***	
Tu	-1.6043 [a]	[-1.8372, -1.3713]	0.1277 [a]	[0.1190, 0.1364]	-0.00107 [a]	[-0.0012, -0.0009]
BF	-2.0043 [a]	[-2.2781, -1.7305]	0.0894 [a]	[0.0665, 0.1122]	-0.00037 [a]	[-0.0008, 0.00003]
TeDF	-2.4286 [a]	[-2.7959, -2.0612]	0.0923 [a]	[0.0757, 0.1089]	-0.00026 [a]	[-0.0006, 0.00004]
TeW	-1.8958 [a]	[-2.3435, -1.4481]	0.0974 [a]	[0.0716, 0.1232]	-0.00040 [a]	[-0.0008, -0.00002]
TeRF	-2.1544 [a]	[-2.4057, -1.9032]	0.1014 [a]	[0.0773, 0.1255]	-0.00046 [a]	[-0.0008, -0.0001]
TrRF_hi	-2.0173 [a]	[-2.5325, -1.5021]	0.1154 [a]	[0.0956, 0.1352]	-0.00071 [a]	[-0.0010, -0.0004]
TrRF_lw	-2.7493 [a]	[-2.9831, -2.5155]	0.0998 [a]	[0.0879, 0.1117]	-0.00047 [a]	[-0.0007, -0.0003]
PFT						
BlDcTmp	-2.2264 [ab]	[-2.4829, -1.9699]	0.0993 [a]	[0.0829, 0.1158]	-0.00050 [a]	[-0.0008, -0.0002]
BlDcTrp	-2.7270 [ab]	[-3.6757, -1.7782]	0.1125 [a]	[0.0961, 0.1288]	-0.00058 [a]	[-0.0008, -0.0003]
BlEvTmp	-1.8106 [a]	[-2.3349, -1.2864]	0.0896 [a]	[0.0577, 0.1215]	-0.00021 [a]	[-0.0007, 0.0003]
BlEvTrp	-2.6105 [b]	[-2.8366, -2.3844]	0.1022 [a]	[0.0912, 0.1132]	-0.00052 [a]	[-0.0007, -0.0003]
C_3H	-1.7507 [ab]	[-2.0680, -1.4334]	0.1271 [a]	[0.1169, 0.1374]	-0.00110 [a]	[-0.0013, -0.0009]
NlEv	-2.0464 [ab]	[-2.5569, -1.5358]	0.1125 [a]	[0.0934, 0.1316]	-0.00063 [a]	[-0.0009, -0.0004]
SEv	-1.8150 [a]	[-2.4609, -1.1691]	0.0971 [a]	[0.0593, 0.1349]	-0.00047 [a]	[-0.0006, -0.0004]
Global Mean	-2.2276	[-2.3966, -2.0586]	0.1012	[0.0921, 0.1104]	-0.00050	[-0.0006, -0.0004]

Biomes and numbers of species (*n*) include tundra (Tu, *n* = 20), boreal forest (BF, *n* = 25), temperate deciduous forest (TeDF, *n* = 10), temperate woodland (TeW, *n* = 67), temperate rainforest (TeRF, *n* = 12), high elevation tropical rainforest (TrRF_hi, *n* = 16), and low elevation tropical rainforest (TrRF_lw, *n* = 81); PFTs include broadleaf deciduous temperate (BlDcTmp, *n* = 40), broadleaf deciduous tropical (BlDcTrp, *n* = 4), broadleaf evergreen temperate (BlEvTmp, *n* = 38), broadleaf evergreen tropical (BlEvTrp, *n* = 88), C_3 herbaceous (C_3H, *n* =13), needle-leaf evergreen (NlEv, *n* = 13), and evergreen shrubs (SEv, *n* = 35). Values were calculated using natural-log-transformed rates of leaf respiration *R*-*T* curve data available from the ~10-45°C curve range. The global mean value was calculated aggregating all individual species parameter values. To determine the effect Biome and PFT groups, we used a mixed-model that nested random effects terms, with Species nested in Site when evaluating Biome, and Species as a single random effect to evaluate the fixed effect of PFT. Post-hoc comparisons based on least-square means determine differences between Biome and PFT groups; differences are noted by unshared letters. Confidence intervals were calculated from individual species' curves.

Figure 1

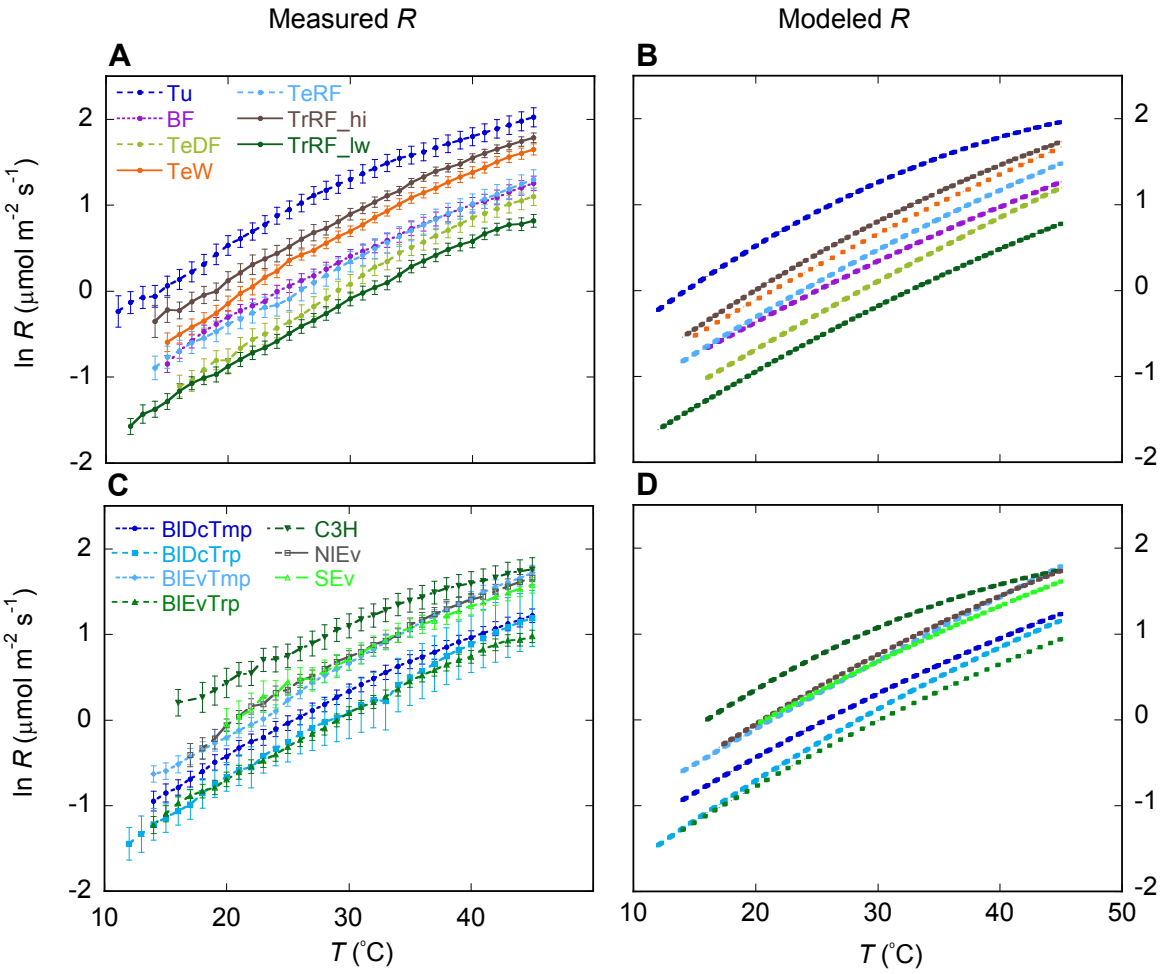
Measured R
Modeled R
A
B
C
D
Tu
BF
TeDF
TeW
TeRF
TrRF_hi
TrRF_lw
BlDcTmp
BlDcTrp
BlEvTmp
BlEvTrp
C3H
NlEv
SEv
ln R (μmol m-2 s-1)
T (°C)

Figure 2

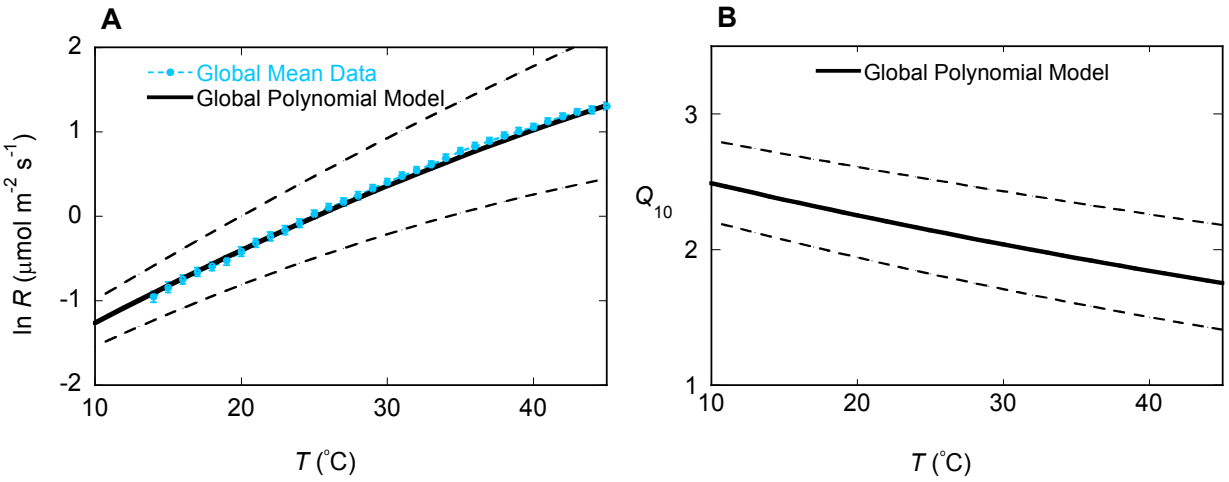
A
Global Mean Data
Global Polynomial Model
ln R (μmol m-2 s-1)
T (°C)
B
Global Polynomial Model
Q10
T (°C)

Figure 3

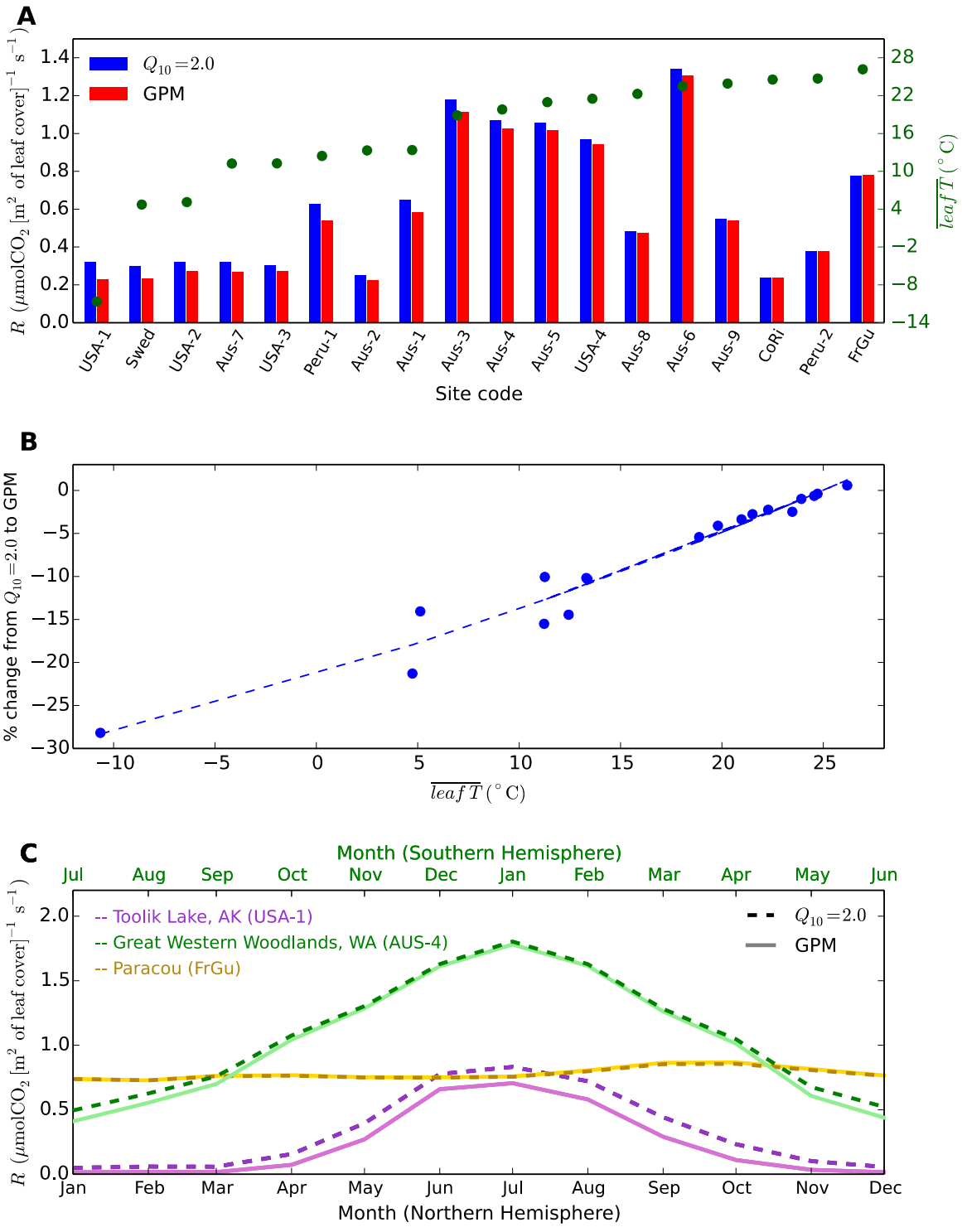
A
Q_{10}=2.0
GPM
R (μmolCO$_2$ [m^2 of leaf cover]$^{-1}$ s^{-1})
$\overline{leaf\,T}$ (°C)
USA-1
Swed
USA-2
Aus-7
USA-3
Peru-1
Aus-2
Aus-1
Aus-3
Aus-4
Aus-5
USA-4
Aus-8
Aus-6
Aus-9
CoRi
Peru-2
FrGu
Site code
B
% change from Q_{10}=2.0 to GPM
$\overline{leaf\,T}$ (°C)
C
Month (Southern Hemisphere)
Jul
Aug
Sep
Oct
Nov
Dec
Jan
Feb
Mar
Apr
May
Jun
-- Toolik Lake, AK (USA-1)
-- Great Western Woodlands, WA (AUS-4)
-- Paracou (FrGu)
Q_{10}=2.0
GPM
R (μmolCO$_2$ [m^2 of leaf cover]$^{-1}$ s^{-1})
Jan
Feb
Mar
Apr
May
Jun
Jul
Aug
Sep
Oct
Nov
Dec
Month (Northern Hemisphere)

Supporting Information

Materials and Methods

Quantification of R-T curves and model comparison

The main objective of this study was to assess how leaf *R* responds to *T* experienced across their current environmental range within the growing season. For this reason, we limited the *T* range of replicate curves evaluated in this study to 10-45°C. Though it is possible that *T* experienced by leaves may exceed this range, especially in arctic tundra and hot, arid woodland ecosystems, 10-45°C approximately spans the mean *T* of the warmest quarter (i.e. warmest 3-month period) for all sites presented in this study (Table S1).

Before analyzing *T* responses of *R* across biomes and plant functional types, we needed to determine which model would best describe the nuances of this response. Physiological model representations of plant respiratory *T* response can vary in their complexity and ability to account for observed biological patterns, such as decreases in the *T* sensitivity of *R* over increasing *T*s. For example, Arrhenius and fixed-Q_{10} exponential equations, which are widely utilized in many TBMs (6, 7) and feature little or no *T*-sensitivity of the *R*-*T* response across biologically relevant *T* ranges. Thus, these models, and the Universal Temperature Dependence (UTD) model (15) (which provides a nearly identical response as the Arrhenius) tend to over-predict *R* rates at low and high *T*s when compared to observed *R* data (Extended Data Fig. 1). The Lloyd & Taylor (17) model contains a modified activation energy parameter to improve the representation of *R* in Arrhenius-based physiological models by allowing for a *T*-variable response. An *R*-*T* model presented by Tjoelker *et al.* integrates the *T*-dependence of *R* more explicitly, which accounts for a predictable *T*-variable Q_{10} shared among species representing several diverse environments (16). To date, data available to rigorously test alternative empirical model fits were typically constrained by low resolution and a narrow range of measurement *T*s, and were further limited by species sample sizes when testing for biomes and PFTs differences. Generally, the inclusion of a *T*-variable Q_{10} to model the *T*-response of *R* substantially improves predicted estimates of *R* (Fig. S1) compared to models that do not include this parameter (*i.e.* Arrhenius, UTD, exponential fixed-Q_{10}) and to models whose *T*-variable parameter effect is less pronounced (i.e.

Lloyd & Taylor). Recent high-resolution *T*-response curves for a single species (27) were consistent with the general shape of the *T*-variable Q_{10} (5).

Exponential fixed-Q_{10}:

$$R = R_{Tref} * Q_{10}^{\frac{T-Tref}{10}}$$

where R_{Tref} is the rate of *R* at chosen reference *T* (T_{ref}, in °C) and Q_{10} is a fixed value.

Arrhenius

$$R = R_{Tref} * e^{\left[\frac{Ea}{(r*Tref)}*(1-\frac{Tref}{T})\right]}$$

where R_{Tref} is the rate of *R* at chosen reference *T* (T_{ref}, in K), *Ea* is an activation energy and *r* is the gas law constant, 8.314 J mol^{-1} K^{-1}.

UTD

$$R = R_0 * e^{\left[\frac{Ei*T}{kT_0{}^2*(1+(\frac{T}{T0}))}\right]}$$

where R_0 is the rate of *R* at 273K (T_0), *Ei* is an activation energy and *k* is Boltzmann's constant, 8.61733 x 10^{-5} eV K^{-1}.

Lloyd & Taylor

$$R = R_{Tref} * e^{Eo\left[\frac{1}{(Tref-T0)}-\frac{1}{T-T0}\right]}$$

where R_{Tref} is the rate of *R* at chosen reference *T* (T_{ref}), *Eo* is an activation energy, and T_0, which is a temperature between *T* and 0K.

Variable-Q_{10}

$$R = R_{Tref}(x-y) * (\frac{T+T_{ref}}{2})^{\frac{T-Tref}{10}}$$

where R_{Tref} is the rate of R at chosen reference T (T_{ref}), and x and y are constants that describe the temperature dependence of Q_{10}.

Finally, the Polynomial Model (Eq. 1), where a, b, and c are fit coefficients from the second order polynomial applied to ln-transformed R.

Over all the replicates available, we assessed the mean residuals produced from each model at each T, from 10-45ºC (Fig. S2a). The Arrhenius model and UTD models produced identical fits, due to their similar structure and use of a single activation energy value; for this reason, we treat their response as identical for comparisons (Fig. S2a). We found a pronounced difference between models that included a T-dependent parameter or allowed for T-sensitivity of the T-response (variable-Q_{10}, polynomial, and to a lesser degree Lloyd & Taylor), and models that did not (exponential fixed-Q_{10}, Arrhenius/UTD), mainly in their ability to fit R at low Ts. Overall, the models that allowed for the most T-sensitivity – the variable-Q_{10} and the polynomial – provided the lowest mean residuals considering all Ts. These results were also seen when fitting all models to the mean R response of individual biomes and plant functional type groups, as well as with the mean R response of all species. Between the variable-Q_{10} and polynomial models, the polynomial model is further removed from the dependence on the concept of Q_{10} formulation, which can be problematic in applying in larger biosphere models, and further, it does not rely on biologically-based assumptions of activation energies. For these reasons we selected to use the polynomial model when comparing the global database of R-T response curves. It should be noted that the main conclusion of this study – the global convergence in T response of leaf R – would still be supported if we chose other models that allow for T-dependent changes in the R-T response (i.e. variable-Q_{10} or Lloyd & Taylor, data not shown); however, the polynomial fit provides the least error across the T range.

Thus, based on the results of model comparison between the commonly applied R-T model functions on all replicates, we confirmed results found in O'Sullivan et al. (27) that a 2nd order polynomial can best represent how R (here, log transformed) responds to T between 10-45˚C. The polynomial fit of the replicate T response curves (Eq. 1) provides three coefficients: a, the y-

axis intercept; *b*, the value of the slope when $T = 0$ °C; and *c*, which determines the decline in the slope (i.e. curvature) with increasing measuring *T*. Thus, each replicate fitted *T* response curve provides a specific *a*, *b*, and *c* value.

Tests for normality and outlier removal

The total number of *T* response curves of *R* originally collected across all field campaigns was 787, though ~40 measured replicate curves were not included in initial analysis due to measurement error caused by instability of the measurement equipment under hot conditions. Replicate measurements were removed from the remaining dataset prior to analysis when values of *R* at 25 °C (area- and mass-based), and values of Q_{10} at 25°C and 10°C were found to be greater or less than two times the interquartile range of all values (values were log-transformed for normality when necessary). Following that filter for outliers, replicates where values of *b* and *c* exceeded more than two times the interquartile range of all remaining values were removed. The final dataset consisted of 673 replicate measured *R* temperature-response curves resulting in a total of 231 individual species-site means, which were used for data analysis.

Segmented interval analysis

Our study aimed to compare the *T* response of *R*, measured at high-resolution between 10 and 45°C across species representing diverse ecosystems and plant forms and functional types. Collecting these response curves under field conditions can sometimes restrict the minimum *T* reached prior to curve measurement initiation due to limitations in the ability of the peltier cooling system of the leaf cuvette to reach 10°C, especially in hot climates. While the rate of warming and reaching of high temperatures were not restricted by the field site environmental conditions, the starting *T* was often ~5°C above 10°C for measurements made at the hotter sites. For this reason, there is some variability in the low, starting *T* of replicate curves.

The variation in starting *T* values between curves posed a potential issue when comparing curves of different ranges (i.e. 10-45 °C, 17-45 °C, 24-45 °C, etc), and their resulting *a*, *b*, and *c* parameters. To address this issue, we performed a 'segmented interval analysis', wherein each replicate curve was divided into 20°C length segments (10-30°C, 15-35°°C, 20-40°C, and 25-

45°C) and a polynomial fit was applied to each segment (Fig. S3). The values of *a*, *b*, and *c* derived from each segmented interval where then compared to each other and the *a*, *b*, and *c* values derived from the original, full-length, non-segmented curve that included the maximum amount of data (Table S2). A mixed-model analysis, which accounted for the unbalanced dataset and potential random effects of Biome and PFT, indicated that none of the parameter values derived from the distinct, 20°C segments differed significantly from the parameter values from response curves that contained all data available (Table S2). While there was some variation between distinct segmented intervals, the lack of significance between any segment and the full length curve supported our use of the full curves, as they provided the most information for a given replicate without compromising comparisons between curves of different lengths.

Ecologically relevant parameters

In addition to the full measured *T* range (10-45°C), we also calculated polynomial parameters *a*, *b*, and *c*, for an 'ecologically relevant' *T* range - a 20°C span centered around the mean *T* value of the warmest quarter at the sampling site, which represents an approximation of growing season *T* range. The parameters for the 'ecologically relevant' *T* range (Table S3) follow similar patterns in variation amongst intercept values (*a*) as those calculated using the 'Full *T* range', and maintain no difference in *b* and *c* between biome or PFT groups, suggesting the fundamental response curve shape is unaffected by measurement *T* range. Thus, despite differences among biomes and PFTs in the offset, the shared shape and curvature of the response of *R* to *T*, as defined by the *b* and *c* model parameters, did not differ significantly, whether over the full *T* range or the 'ecologically relevant' *T* range (Table 1 and S3).

Parameterizing JULES for modeling leaf-R

The JULES model is the land surface description for the current UK Hadley Centre HadGEM family of Global Circulation Models (28). Two key requirements placed on the model are to determine the split of surface available energy into sensible and latent heat fluxes, and to calculate terrestrial carbon cycling and thus the role of ecosystems in the changing global carbon cycle. The two calculations are coupled, as in one configuration JULES can operate with a

Dynamic Global Vegetation Model (DGVM) component; TRIFFID (28, 53). Climatically induced changes to leaf components such as stomatal opening can alter net primary productivity, which in turn can feedback on energy partitioning via DGVM projections of altered Leaf Area Index (LAI).

The JULES model is also available independent of a GCM, and as a fully offline description of terrestrial response. Our descriptions of leaf *R* could be modeled completely independent of any land surface model, if leaf-level temperature is known throughout our years of interest. In general this quantity is unavailable, and so the main purpose of our JULES simulations is to generate leaf *T* values resulting from the WFDEI-based estimated mean screen-level meteorological conditions (41). Leaf level *T* is a diagnostic from the JULES solution to the surface energy balance, a consequence of solution to a form of the Penman-Monteith equation (54). This value will depend on parameters set, including LAI (28). In our configuration, as LAI is known at each site, this value is prescribed although it is allowed to change as the model is extrapolated to other seasons to capture phenology on leaf cover – hence the "dynamic" component of TRIFFID is overridden.

Further, in other applications of JULES, leaf *R* varies through the canopy, and then the energy balance will create different leaf *T* values through the canopy due to changing light levels. As we are interested in leaf-level response of fully sun exposed leaves, for this run we ignore intra-canopy variability in the resulting *R* values. That is, a "tree" of LAI of unity, and with no self-shading. The exception to this is inclusion of phenology, where we normalized leaf *R* by $LAI(t)/LAI_M$, where *t* is time, LAI(*t*) is modeled LAI based only on phenological changes, and LAI_M is maximum, prescribed LAI.

Supporting Information References:

44. Huntingford C, Cox PM, & Lenton TM (2000) Contrasting responses of a simple terrestrial ecosystem model to global change. *Ecological Modelling* 134(2000):41-58.

45. Monteith JL (1981) Evaporation and surface temperature. *Quarterly Journal of the Royal Meteorological Society* 107(451):1-27.

46. Hijmans RJ, Cameron SE, Parra JL, Jones PG, & Jarvis A (2005) Very high resolution interpolated climate surfaces for global land areas. *International Journal of Climatology* 25:1965-1978.

Table S1. Geographic, climatic, and sampling information of field sites from which leaves were sampled for measurement.

Biome	Dates of measurement	Lat. (°*N*)	Long. (°*E*)	Elevation (*m.a.s.l.*)	MAT (°*C*)	TWQ (°*C*)	Annual precip. (*mm*)	Aridity index	PFTs represented	No. Species	No. total reps	Fig. 3A site code
Tundra												
Toolik Lake, AK, USA	June 2010	68.63	-149.6	720	-11.3	8.2	225	0.61	C3H, BIDcTmp, SEv, NIEv	20	79	USA-1
Boreal Forest												
Umea, Sweden	Aug. 2013	63.821	20.311	29	2.5	14.3	579	1.13	BIDcTmp, NIEv	10	37	Swed
Ely, MN, USA	July 2013	47.956	-91.75	420	3.2	17.6	703	0.9	BIDcTmp, NIEv	15	59	USA-2
Temperate Deciduous Forest												
Black Rk Forest, NY, USA	June 2013	41.408	-74.012	335	7.43	19.52	1103	1.17	BIDcTmp	10	38	USA-3
Temperate Woodland												
Aranda, ACT, AUS	Sept. 2011	-35.275	149.079	580	12.7	19.5	682	0.55	BIEvTmp	10	33	AUS-1
ANU campus, ACT, AUS	March 2012	-35.279	149.108	571	13.1	19.8	637	0.51	BIDcTmp	4	15	AUS-2
Calperum, SA, AUS	March 2013	-34.037	140.674	35	17.25	23.6	255	0.17	SEv, BIEvTmp, NIEv	16	34	AUS-3
College Station, TX, USA	Oct. 2010	30.6	-96.400	103	20	28.5	995	0.68	BIDcTmp, NIEv	2	8	USA-4
Great Western Woodlands, WA, AUS	April 2013	-30.264	120.692	459	18.5	25.6	273	0.18	SEv, BIEvTmp, NIEv, C3H	16	41	AUS-4
Jurien Bay, WA, AUS	Nov. 2011	-30.241	115.071	23	18.87	23.83	558	0.39	BIDcTmp, SEv, C3H, BIEvTmp	15	56	AUS-5
Alice Mulga, NT, AUS	Feb. 2012	-22.283	133.249	607	22.4	28.9	321	0.17	BIEvTmp, SEv	4	6	AUS-6
Temperate Rain Forest												
Warra, TAS, AUS	March 2012	-43.095	146.724	86	10.78	14.43	1380	1.69	BIEvTmp, SEv	12	45	AUS-7
Tropical Rainforest (high altitude)												
Wayquecha, Peru	Sept. 2011	-13.19	-71.587	3000	13.4	14.5	335	0.23	BIEvTrp	16	17	PERU-1
Tropical Rainforest (low altitude)												
San Isidro Costa Rica	July 2011	10.38	-84.620	479	24	25	4045	2.61	BIEvTrp, SEv	5	16	CoRi
Atherton, QLD, AUS	Aug. 2012	-17.12	145.632	728	21	23.8	2140	1.47	BIEvTrp	16	58	AUS-8
Cape Tribulation, FNQ, AUS	Sept. 2010	-16.28	145.480	90	25.2	27.5	2087	1.39	BIEvTrp	12	35	AUS-9
Paracou, French Guiana	Oct. 2010	5.27	-52.920	21	25.8	26.2	2824	1.88	BIEvTrp, BIDcTrp	32	76	FrGu
Iquitos, Peru	Sept. 2011	-3.949	-73.434	114	25.3	26.8	2769	1.64	BIEvTrp	16	16	PERU-2

The aridity index is the quotient of mean annual precipitation divided by mean annual evapotranspiration (55).

Table S2. Mean values (+/- S.D.) of coefficients (*a, b*, and *c*) of polynomial models of the ln *R-T* response, calculated for four 20˚C segmented intervals across the full-measurement range of the response for all replicate curves (*n*=673).

Segmented Interval Range	*n*	*a*	S.D.		*b*	S.D.		*c*	S.D.	
10-30 °C	346	-2.1001	1.2962	a	0.0969	0.0944	a	-0.00044	0.00210	a
15-35 °C	523	-2.1539	1.3440	ab	0.0979	0.0896	a	-0.00045	0.00169	a
20-40 °C	623	-2.1203	1.8446	a	0.0964	0.1168	a	-0.00042	0.00189	a
25-45 °C	599	-2.3610	1.4938	b	0.1163	0.0764	b	-0.00076	0.00108	b
Complete available *T* range	673	-2.2003	1.3559	ab	0.1034	0.0715	ab	-0.00055	0.00110	ab

Values of *a, b*, and *c* parameters were statistically compared individually using a mixed-model with the segmented interval range as a fixed-effect, and nests the random effects of Biome and PFT for each replicate. This approach accommodates the unbalanced dataset across the interval ranges. Significant variation between parameters by segment range is marked with unshared letters. Parameter values calculated from ln *R-T* curves that include all available data are not significantly different than any parameter values calculated from individual 20°C segmented intervals, justifying our use of all available data for the calculation of coefficient values.

Table S3. 'Ecologically relevant' mean *a*, *b* and *c* parameter values and 95% confidence intervals (in brackets) of biomes and plant functional types (PFTs) across all species.

Biome	***a***		***b***		***c***		***n***
Tu	-1.6297 [ab]	[-2.1322, -1.1272]	0.1257 [a]	[0.0869, 0.1645]	-0.00095 [a]	[-0.0018, -0.0001]	20
BF	-1.9455 [ab]	[-2.3502, -1.5409]	0.0836 [a]	[0.0488, 0.1184]	-0.00025 [a]	[-0.0010, 0.0004]	25
TeDF	-1.8827 [ab]	[-2.2722, -1.4931]	0.0423 [a]	[0.0162, 0.0683]	0.00080 [a]	[0.0002, 0.0014]	10
TeW	-1.5478 [a]	[-2.1334, -0.9622]	0.0743 [a]	[0.0357, 0.1130]	0.000002 [a]	[-0.0006, 0.0006]	66
TeRF	-2.0273 [ab]	[-2.4007, -1.6540]	0.0986 [a]	[0.0625, 0.1347]	-0.00051 [a]	[-0.0014, 0.0003]	13
TrRF_hi	-1.9061 [ab]	[-2.4132, -1.3990]	0.0961 [a]	[0.0704, 0.1218]	-0.00056 [a]	[-0.0011, -0.00003]	16
TrRF_lw	-2.7370 [b]	[-3.1060, -2.3679]	0.1070 [a]	[0.0837, 0.1302]	-0.00038 [a]	[-0.0008, 0.00004]	81
PFT							
BlDcTmp	-1.9553 [ab]	[-2.2335, -1.6770]	0.0800 [a]	[0.0578, 0.1022]	-0.00013 [a]	[-0.0006, 0.0003]	40
BlDcTrp	-3.1352 [ab]	[-4.3860, -1.8843]	0.1526 [a]	[0.0821, 0.2230]	-0.00165 [a]	[-0.0038, 0.0005]	4
BlEvTmp	-1.2877 [a]	[-1.9003, -0.6751]	0.0518 [a]	[0.0127, 0.0909]	0.00047 [a]	[-0.0002, 0.0011]	34
BlEvTrp	-2.5695 [b]	[-2.9071, -2.2318]	0.0962 [a]	[0.0756, 0.1168]	-0.00037 [a]	[-0.0007, -0.000001]	92
C_3H	-1.6821 [ab]	[-2.1694, -1.1948]	0.1272 [a]	[0.0928, 0.1615]	-0.00103 [a]	[-0.0017, -0.0004]	13
NlEv	-1.7876 [ab]	[-2.6843, -0.8909]	0.0864 [a]	[0.0148, 0.1579]	-0.00013 [a]	[-0.0015, 0.0005]	13
SEv	-1.8495 [ab]	[-2.7611, -0.9379]	0.1003 [a]	[0.0390, 0.1616]	-0.00054 [a]	[-0.0015, 0.0005]	35
Global Mean	-2.0812	[-2.3137, -1.8487]	0.0897	[0.0747, 0.1046]	-0.00027	[-0.0005, -.00001]	231

Biomes and PFTs are listed in the text of Table 1. The parameters were calculated from a 20°C interval of the *R*-*T* response curve that best represents *T*s experienced by an individual species at the site from which it was sampled, based on the mean *T* of the warmest quarter (55) therefore referred to as the 'Ecologically relevant *T* range'. The global mean value was calculated considering all species parameter values equally. To determine the influence of Biome and PFT on the parameter values, we used a mixed-model that nested random effect terms, with Species nested in Site when evaluating Biome, and with nested Species as a random effect when evaluating PFT. Significant differences across biomes and PFT groups were evaluated by a post-hoc comparison of least-square means, and are indicated by unshared letters. 'Ecologically relevant' values of these parameters are not statistically significantly different from the 'Full *T* range' parameter values (Table 1), as determined by a separate mixed-model analysis, with Site nested in Biome, and Species nested in PFT.

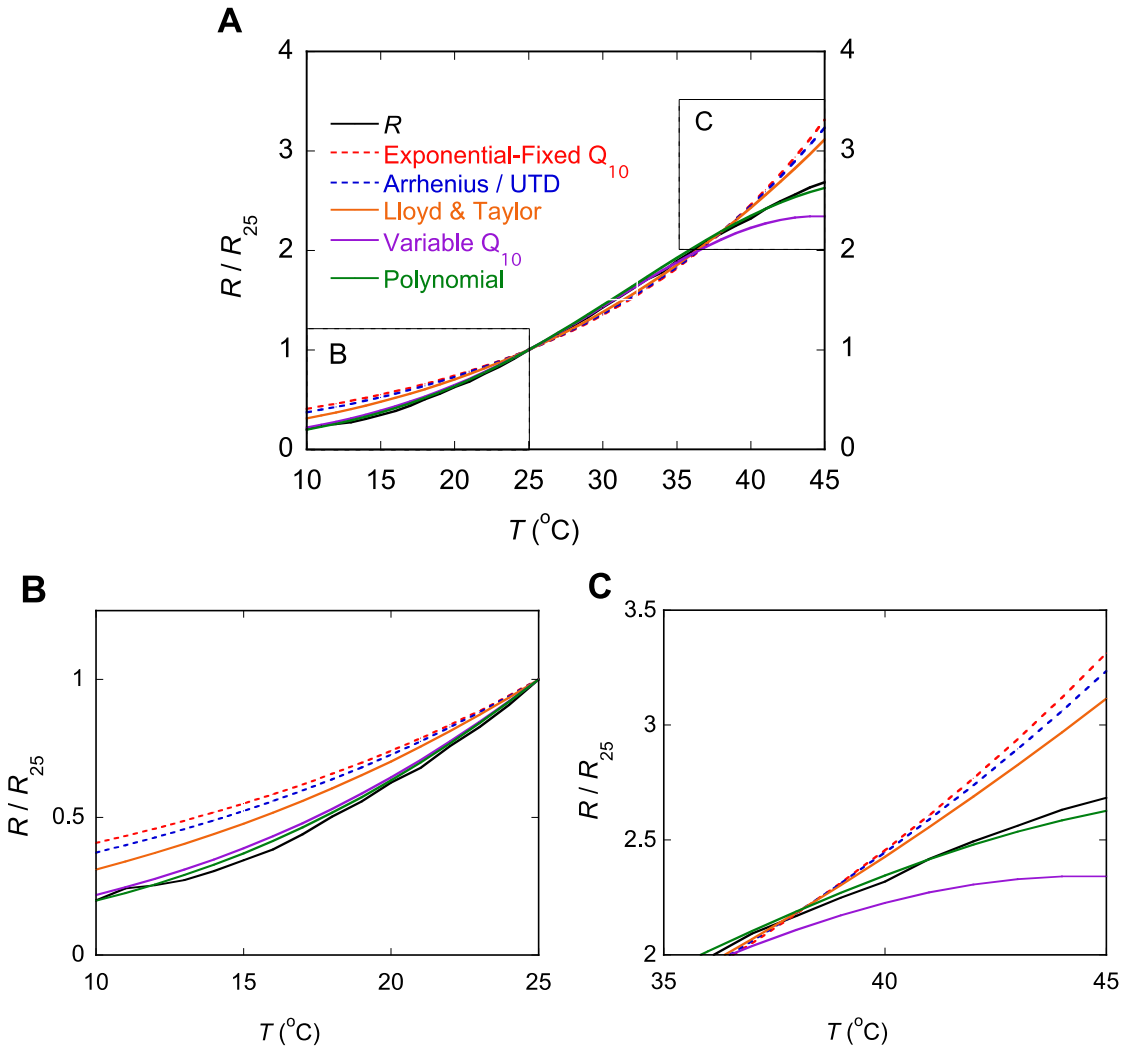

Figure S1. An example temperature (*T*) response curve of respiration (*R*) from 10-45ºC, normalized to the rate of *R* at 25ºC (solid black line), displayed with commonly applied functional models of the *T*-response (also normalized to 25ºC) that vary in their characterization of *R* (A) Functional models that do not account for the temperature-dependent *T*-sensitivity of the *R*-*T* response (Exponential-Fixed Q_{10}, Arrhenius / UTD(15)) are represented with dashed lines, and models that do account for this sensitivity (Lloyd & Taylor(17), Variable Q_{10} (12, 16), and Polynomial(27)) are shown with solid lines. Differences between the functional models are more pronounced at *T*s below 20ºC (B) and above 40ºC (C).

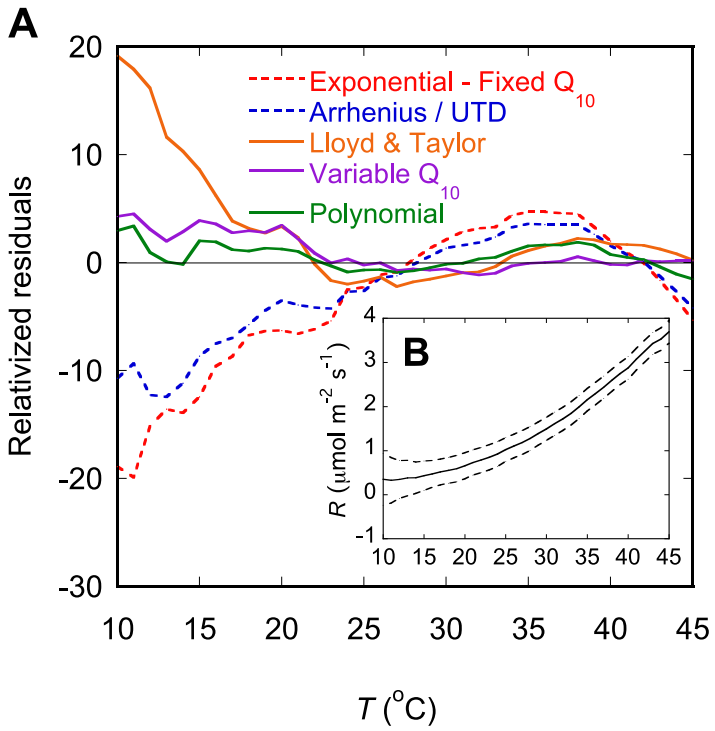

Figure S2. Mean relativized residuals (percent error in prediction) of estimates of commonly applied models based on all replicate *R-T* response curves. All replicates (n = 673 leaves) across 10-45ºC (**a**) highlight the significance of T-dependent parameter inclusion, as seen in the variable-Q_{10} and polynomial fits (solid lines) in contrast to the fixed-T sensitivity models (broken lines). The global mean response of R to T across all species measured in this study (**b**, inset, n = 231) are bracketed by 95% CI (dashed lines).

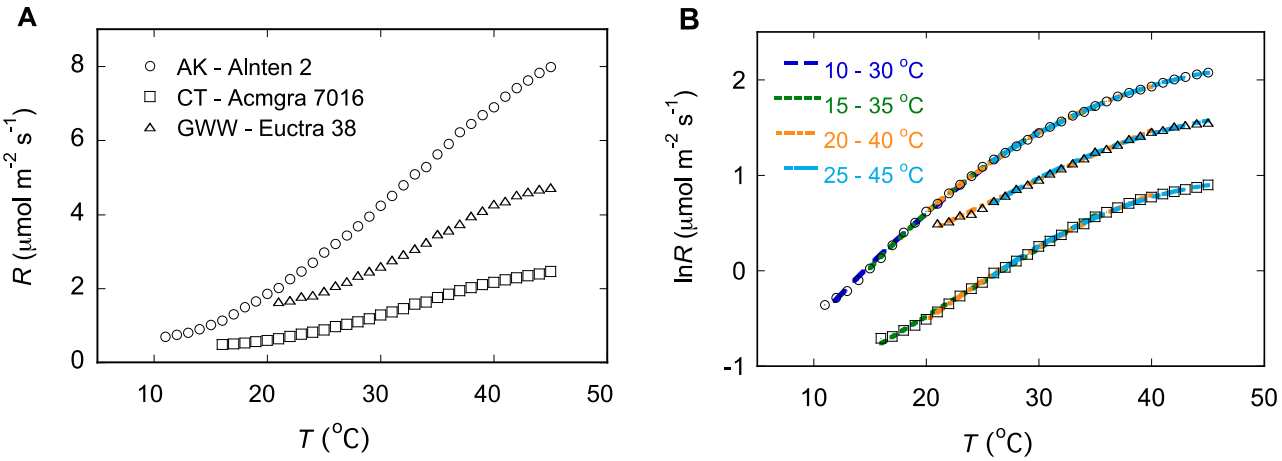

Figure S3. Segmented interval approach to polynomial model analysis. Three representative leaf respiration (*R*)- temperature response curves (A) of replicate leaves of sampled species from Toolik Lake, Alaska, USA (AK; *Alnus tenufolia*), Cape Tribulation, Far North Queensland, AUS (CT; *Acmena graveolens*), and Great Western Woodlands, Western Australia sites (GWW; *Eucalyptus transcontinentalis*). To assess the effect of measurement *T* range variation in *a*, *b*, and *c* parameters calculated from the log-polynomial fit, we used a "segmented interval" approach (B). The segmented interval approach fit polynomial curves across 20ºC range intervals of replicate ln *R* data, specifically 10-30 ºC (blue), 15-35 ºC (green), 20-40 ºC (orange), and 25-45 ºC (light blue) as shown in panel (B). The resulting *a*, *b*, and *c* parameters calculated from these segmented intervals were then statistically compared to each other, and to the *a*, *b*, and *c* values resulting from a polynomial fit that included the entire range of data available from the original measured *R*-*T* replica

Table S4. Polynomial parameter values of all species included in analysis, grouped by biome and site. Plant functional type (PFT) is identified for each species. The polynomial curve fit parameters for each species at each site is presented, for both the full fit using all available data from the *R*-*T* response curve measurement, and for a 20ºC segment of the *R*-*T* response curve representing an ecologically meaningful *T* range. An asterisk (*) denotes the use of the next closest 20ºC segment for the ecologically relevant *T* range when the most appropriate segment was unavailable given the data from the original curve. The number of replicate measurements made for each species (*n*) is shown in the far right column.

Biome/Site	Species	PFT	All data available *T* range			Ecologically meaningful *T* range				*n*
Tundra			***a***	***b***	**c**	***a***	***b***	**c**		
Toolik Lake, AK, USA							**10-30 ºC**			
	Arnica alpina	C3H	-1.9003	0.1219	-0.00119	-1.7136	0.0980	-0.00050		4
	Alnus tenuifolia	BlDcTmp	-2.1640	0.1657	-0.00163	-2.5618	0.1997	-0.00231		4
	Anemone narcissiflora	C3H	-1.9126	0.1541	-0.00166	-1.0177	0.1284	-0.00148	*	5
	Arctostaphylos alpina	BlDcTmp	-1.4768	0.1115	-0.00086	-1.2844	0.0938	-0.00041		3
	Astragalus umbellatus	C3H	-1.4413	0.1365	-0.00123	-1.0394	0.0920	-0.00019		4
	Cassiope tetragona	SEv	-1.9700	0.1106	-0.00085	-2.1632	0.1232	-0.00104		5
	Dryas octopetela	SEv	-1.7594	0.1735	-0.00179	-4.4573	0.3383	-0.00472		4
	Empetrum nigrum	SEv	-2.6064	0.1349	-0.00105	-0.4779	-0.0475	0.00307		4
	Epilobium latifolium	C3H	-1.2596	0.1265	-0.00111	-1.1172	0.1132	-0.00075		4
	Eriophorum angustifolium	C3H	-1.9139	0.1164	-0.00078	-1.8115	0.1054	-0.00051		4
	Ledum palustre	SEv	-0.8136	0.1127	-0.00068	-0.7913	0.1100	-0.00062		3
	Pedicularis capitata	C3H	-1.0286	0.1208	-0.00113	-0.9162	0.1094	-0.00087		4
	Picea glauca	NlEv	-0.7909	0.1110	-0.00062	0.0453	0.0039	0.00204		4
	Polygonum bistorta	C3H	-0.7664	0.1154	-0.00099	-0.6725	0.1045	-0.00071		4
	Populus balsamifera	BlDcTmp	-1.5489	0.1265	-0.00110	-1.4311	0.1126	-0.00072		4
	Potentilla nivea	C3H	-1.9075	0.1302	-0.00118	-4.1282	0.3230	-0.00472		3
	Rhododendron lapponicum	BlDcTmp	-2.3657	0.1367	-0.00101	-2.0358	0.0955	-0.00008		4
	Rubus chamaemorus	C3H	-1.6090	0.1436	-0.00143	-1.3039	0.1118	-0.00068		4
	Salix reticulata	BlDcTmp	-0.9819	0.0975	-0.00051	-0.9173	0.0880	-0.00023		4
	Vaccinium vitis-ideae	BlDcTmp	-1.8687	0.1074	-0.00067	-2.7988	0.2108	-0.00355		4
Boreal Forest										

Umea, Sweden						**10-30 ºC**			
	Vaccinium myrtillus	BIDcTmp	-0.2512	-0.1411	0.00373	-0.0849	-0.1552	0.00398	2
	Betula nana	BIDcTmp	-2.0304	0.1032	-0.00081	-2.0857	0.1007	-0.00080	4
	Salix caprea	BIDcTmp	-2.5727	0.1404	-0.00115	-2.1867	0.1283	-0.00107	4
	Pinus sylvestris	NIEv	-1.0969	0.0701	-0.00001	-0.7587	0.0308	0.00100	4
	Alnus icana	BIDcTmp	-1.2662	0.0407	0.00039	-0.7611	-0.0162	0.00181	4
	Betula pendula	BIDcTmp	-2.4912	0.0929	-0.00025	-2.8395	0.1317	-0.00125	3
	Picea abies	NIEv	-2.0531	0.1133	-0.00065	-2.3557	0.1428	-0.00138	4
	Vaccinium vitus	BIDcTmp	-1.0555	0.0199	0.00059	-1.2049	0.0312	0.00044	4
	Populus tremula	BIDcTmp	-2.9989	0.1393	-0.00110	-3.0275	0.1587	-0.00160	4
	Calluna vulgaris	BIDcTmp	-1.2378	0.0868	-0.00036	-0.8020	0.0469	0.00068	4
Ely, MN, USA						**10-30 ºC**			
	Fraxinus nigra	BIDcTmp	-1.4356	0.0567	0.00013	-0.5135	-0.0203	0.00165 *	3
	Betula papifera	BIDcTmp	-2.4348	0.1155	-0.00092	-2.7470	0.1499	-0.00174 *	4
	Populus tremuloides	BIDcTmp	-2.3407	0.0985	-0.00050	-1.4438	0.0189	0.00130	4
	Acer rubrum	BIDcTmp	-2.3407	0.0985	-0.00050	-1.4438	0.0189	0.00130	4
	Populus balsam	BIDcTmp	-2.5001	0.1367	-0.00142	-2.1929	0.1119	-0.00093	4
	Abies balsam	NIEv	-3.1896	0.1691	-0.00168	-3.9463	0.2350	-0.00303 *	4
	Thuja occidentalis	NIEv	-1.9832	0.1271	-0.00107	-1.5735	0.0927	-0.00034	4
	Pinus strobus	NIEv	-2.2607	0.1123	-0.00072	-3.0102	0.1854	-0.00264	4
	Pinus banksiana	NIEv	-1.3082	0.0585	0.00026	-0.9010	0.0202	0.00108	4
	Alnus rugosa	BIDcTmp	-2.4043	0.0854	-0.00030	-2.2306	0.1041	-0.00096	4
	Corylus cornuta	BIDcTmp	-2.4394	0.1015	-0.00071	-2.2531	0.1078	-0.00113	4
	Diervilla lonicera	BIDcTmp	-2.9152	0.1137	-0.00080	-2.9369	0.1230	-0.00106 *	4
	Larix laricina	NIEv	-1.9624	0.0793	-0.00015	-2.7836	0.1395	-0.00146 *	5
	Picea mariana	NIEv	-1.7913	0.1199	-0.00090	-3.6048	0.2310	-0.00299	4
	Picea glauca	NIEv	-1.7470	0.0956	-0.00038	-0.9507	-0.0271	0.00283	3
Temperate Deciduous Forest									
Black Rock Forest, NY, USA						**10-30 ºC**			
	Populus tremuloides	BIDcTmp	-2.7105	0.0663	0.00061	-2.2238	0.0250	0.00141	4
	Carya glabra	BIDcTmp	-3.2114	0.1398	-0.00089	-2.3682	0.0839	0.00001	5

Liliodendren tulipifera	BlDcTmp	-3.0140	0.1274	-0.00095	-2.0939	0.0617	0.00034		5
Quercus rubra	BlDcTmp	-2.1856	0.0770	0.00013	-1.3596	0.0296	0.00075		4
Acer saccharum	BlDcTmp	-2.9497	0.1136	-0.00058	-2.3212	0.0518	0.00083		3
Acer rubrum	BlDcTmp	-2.5504	0.1043	-0.00049	-1.2108	-0.0424	0.00294		4
Quercus prinus	BlDcTmp	-1.9351	0.0751	-0.00011	-1.5395	0.0291	0.00106		4
Betula papifera	BlDcTmp	-1.4458	0.0687	-0.00027	-1.5601	0.0674	0.00001		2
Populus grandidentata	BlDcTmp	-1.6903	0.0777	-0.00004	-1.0883	0.0097	0.00149	*	4
Betula lenta	BlDcTmp	-2.5929	0.0731	0.00000	-3.0612	0.1068	-0.00085		3
Temperate Woodland									
Aranda, ACT, AUS						**10-30 °C**			
Eucalyptus blakelyi	BlEvTmp	-1.5723	0.0930	-0.00032	-1.4216	0.0756	0.00012		3
Eucalyptus bridgesiana	BlEvTmp	-2.0647	0.1138	-0.00074	-1.9101	0.0950	-0.00027		3
Eucalyptus dives	BlEvTmp	-1.3507	0.0633	0.00006	-1.4187	0.0608	0.00029		3
Eucalyptus macrorhyncha	BlEvTmp	-1.3916	0.0774	0.00000	-1.3884	0.0780	-0.00004		4
Eucalyptus mannifera	BlEvTmp	-0.8306	0.0461	0.00035	-0.6669	0.0265	0.00084		3
Eucalyptus melliodora	BlEvTmp	-1.5343	0.0771	-0.00003	-1.7622	0.0935	-0.00030		3
Eucalyptus pauciflora	BlEvTmp	-1.7555	0.1119	-0.00080	-1.6504	0.1016	-0.00060		3
Eucalyptus polyanthemos	BlEvTmp	-1.5995	0.0786	-0.00005	-1.3688	0.0537	0.00054		4
Eucalyptus rossii	BlEvTmp	-1.4454	0.0674	-0.00004	-1.5388	0.0768	-0.00024		3
Eucalyptus rubida	BlEvTmp	-1.7403	0.0970	-0.00040	-1.7759	0.0988	-0.00041		4
ANU campus, ACT, AUS						**10-30 °C**			
Populus nigra 'Italica'	BlDcTmp	-3.7575	0.1681	-0.00144	-4.0238	0.1881	-0.00179	*	4
Populus deltoides	BlDcTmp	-3.8372	0.1725	-0.00150	-3.3009	0.1428	-0.00089		3
Salix sepulcralis 'Chrysocoma'	BlDcTmp	-3.2111	0.1569	-0.00164	-3.4437	0.1778	-0.00207	*	4
Gingko biloba	BlDcTmp	-3.7472	0.1415	-0.00128	-2.3382	0.0547	0.00008		5
Calperum, SA, AUS						**15-35 °C**			
Acacia stenophylla	BlEvTmp	-1.5959	0.0657	0.00013	-0.3923	-0.0057	0.00134	*	3
Alectryon oleifolius	SEv	-1.3331	0.0346	0.00092	0.0955	-0.0618	0.00252	*	1
Beyeria opaca	SEv	-3.8414	0.1885	-0.00157	-5.7543	0.2951	-0.00302	*	1
Callitris gracilis	NlEv	-4.5012	0.1851	-0.00111	1.9808	-0.2471	0.00593	*	2
Danesa brevifolia	SEv	2.0405	-0.0886	0.00207	-3.1869	0.2721	-0.00399		2

	Dodonaea bursariifolia	SEv	-1.4323	0.0861	-0.00052	-1.4469	0.0780	-0.00033	*	2
	Eremophila glabra	SEv	-3.8281	0.2193	-0.00229	-4.1886	0.2446	-0.00272	*	2
	Eucalyptus dumosa	SEv	-0.0393	0.0053	0.00113	0.6025	-0.0407	0.00183	*	3
	Eucalyptus largiflorens	BlEvTmp	-1.5431	0.0784	0.00015	-0.7785	0.0240	0.00109	*	2
	Eucalyptus socialis	BlEvTmp	-0.6571	0.0352	0.00067	0.4020	-0.0419	0.00201	*	2
	Grevillea huegelii	SEv	4.0336	-0.2819	0.00537	8.0851	-0.5664	0.01019	*	1
	Myoporum platycarpum	BlEvTmp	-0.9328	0.0454	0.00037	0.1810	-0.0352	0.00177	*	2
	Senna artemisioides ssp. coriacea	SEv	-0.8773	0.0699	-0.00027	-1.5828	0.1102	-0.00083	*	2
	Senna artemisioides ssp. filifolia	SEv	-2.4214	0.1386	-0.00108	-2.5438	0.1479	-0.00125	*	3
	Templetonia egena	SEv	-0.9752	0.0752	-0.00015	0.0208	-0.0022	0.00108	*	4
	Westringia rigida	SEv	-2.7335	0.1728	-0.00166	-2.6884	0.1698	-0.00161	*	1
College Station, TX, USA							**20-40 ºC**			
	Juniperus virginiana	NlEv	-1.9976	0.1079	-0.00056	-2.9153	0.1726	-0.00165		4
	Quercus stellata	BlDcTmp	-2.5524	0.1216	-0.00081	-2.6530	0.1313	-0.00097		4
Great Western Woodlands, WA, AUS							**15-35 ºC**			
	Acacia aneura	BlEvTmp	-7.8968	0.4074	-0.00452	-5.9628	0.2817	-0.00252	*	1
	Acacia burkittii	BlEvTmp	3.2687	-0.2151	0.00417	6.8609	-0.4699	0.00854	*	1
	Acacia hemiteles	SEv	-2.4129	0.0889	-0.00014	-5.1902	0.2396	-0.00209	*	3
	Atriplex nummularia	SEv	2.6815	-0.2050	0.00378	2.6815	-0.2050	0.00378	*	1
	Maierana triptera	SEv	-2.7814	0.1754	-0.00167	-3.8846	0.2428	-0.00274	*	3
	Sclerolaena dicantha	SEv	-2.7089	0.1626	-0.00152	-2.3048	0.1409	-0.00118	*	3
	Eremophila scoparia	SEv	-3.1067	0.2109	-0.00195	-6.6149	0.4404	-0.00548	*	3
	Eucalyptus clenandii	BlEvTmp	-1.3554	0.0776	-0.00003	0.2226	-0.0327	0.00187	*	4
	Eucalyptus salmonophloia	BlEvTmp	-2.9011	0.1309	-0.00052	-0.9144	0.0136	0.00132	*	4
	Eucalyptus salubris	BlEvTmp	-2.0790	0.1277	-0.00082	-1.0805	0.0628	0.00034	*	3
	Eucalyptus transcontinentalis	BlEvTmp	-2.3496	0.1363	-0.00097	-1.5361	0.0942	-0.00042	*	4
	Exocarpos cupressiformis	NlEv	-1.9208	0.1132	-0.00062	-2.4648	0.1434	-0.00103	*	2
	Maierana sedifolia	SEv	-1.5858	0.0880	-0.00060	3.7553	-0.2852	0.00542	*	1
	Olearia muelleri	SEv	-5.3555	0.2967	-0.00321	-5.6231	0.3123	-0.00343	*	2
	Ptilotus holosericeus	C3H	-1.4769	0.0806	-0.00037	-1.7953	0.1053	-0.00076	*	4
	Ptilotus obovatus	C3H	-2.9326	0.1539	-0.00139	-2.0925	0.0900	-0.00020	*	2

Jurien Bay, WA, AUS						**15-35 °C**			
	Acacia rostellifera	BlDcTmp	-2.0475	0.0952	-0.00045	-2.1130	0.1104	-0.00082	2
	Anthocercis littorea	SEv	-1.6183	0.0986	-0.00067	-1.1732	0.0703	-0.00009	4
	Dioscorea hastifolia	C3H	-2.4703	0.1248	-0.00102	-2.3928	0.1793	-0.00219	4
	Myoporum insulare	BlEvTmp	-3.2569	0.1172	-0.00069	-2.0696	0.0113	0.00156	2
	Spyridium globulosum	SEv	-1.7873	0.0900	-0.00035	-1.5239	0.0680	0.00025	4
	Acacia rostellifera	BlDcTmp	-0.6050	0.0331	0.00037	-0.4352	0.0396	0.00024	4
	Clematis linearifolia	C3H	-2.1399	0.1282	-0.00080	-1.8666	0.0927	0.00013	4
	Opercularia spermacocea	SEv	-2.4639	0.1590	-0.00167	-3.4845	0.2636	-0.00415	4
	Santalum acuminatum	BlEvTmp	-2.1142	0.1526	-0.00163	-1.8508	0.1254	-0.00091	4
	Spyridium globulosum	SEv	-2.1691	0.0887	-0.00032	-2.1653	0.0803	-0.00004	4
	Acacia rostellifera	BlDcTmp	-1.8918	0.1281	-0.00083	-1.2930	0.0929	-0.00016	4
	Anthocercis littorea	SEv	-1.4190	0.1083	-0.00082	-1.3432	0.1028	-0.00073	4
	Banksia prionotes	SEv	-1.7328	0.0882	-0.00031	-1.8970	0.0870	-0.00032	4
	Hakea incrassate	SEv	-1.0918	0.0707	-0.00024	-1.2395	0.0826	-0.00047	* 4
	Scaevola sp.	SEv	-1.3400	0.1119	-0.00091	-1.7276	0.1432	-0.00150	4
Alice Mulga, NT, AUS						**20-40 °C**			
	Eucalypt sp.	BlEvTmp	0.5506	-0.1524	0.00456	-0.9651	-0.0407	0.00257	1
	Eucalyptus camaldulensis	BlEvTmp	-1.1776	0.1110	-0.00049	-1.1776	0.1110	-0.00049	* 3
	Hakea leucoptera	SEv	-6.4097	0.3207	-0.00297	-2.7197	0.1441	-0.00080	* 2
	Psydrax latifola	BlEvTmp	-2.9595	0.2178	-0.00183	-1.7974	0.1599	-0.00117	* 2
Temperate Rainforest									
Warra, TAS, AUS						**10-30 °C**			
	Eucalyptus obliqua	BlEvTmp	-1.8544	0.1109	-0.00057	-1.2336	0.0688	0.00038	4
	Acacia melanoxylon	BlEvTmp	-1.9413	0.0399	0.00098	-0.8100	-0.0652	0.00320	3
	Nothofagus cunninghamii	BlEvTmp	-2.2781	0.0937	-0.00035	-1.3911	0.0329	0.00084	4
	Atherosperma moschatum	BlEvTmp	-2.4191	0.0877	-0.00036	-3.4980	0.1891	-0.00265	4
	Pomaderris apetala	SEv	-2.4299	0.0801	-0.00009	-2.3017	0.1671	-0.00284	4
	Acacia dealbata	BlEvTmp	-1.7258	0.1048	-0.00057	-2.2557	0.1283	-0.00114	3
	Leptospermum lanigerum	BlEvTmp	-2.3674	0.1264	-0.00100	-2.4011	0.1250	-0.00094	4
	Notelaea ligustrina	BlEvTmp	-2.0825	0.1415	-0.00125	-2.1592	0.1080	-0.00037	4

	Tasmannia lanceolata	SEv	-1.9115	0.0820	-0.00021	-1.8607	0.0779	-0.00014	4
	Melaleuca squarrosa	BlEvTmp	-1.6897	0.0762	-0.00025	-1.6509	0.0726	-0.00018	4
	Eucryphia lucida	BlEvTmp	-2.9189	0.1033	-0.00042	-2.6216	0.0844	-0.00006	4
	Phyllocladus aspleniifolius	SEv	-1.4296	0.0542	-0.00004	-2.3743	0.1331	-0.00158	3
Tropical Rainforest (high altitude)									
Wayquecha, Peru							**10-30 ºC**		
	Bejaria aestuans	BlEvTrp	0.5570	0.0543	-0.00070	-0.1414	0.1210	-0.00205	1
	Weinmannia crassifolia	BlEvTrp	-2.1059	0.0991	-0.00040	-1.0773	0.0131	0.00130 *	1
	Escallonia paniculata	BlEvTrp	-1.8666	0.1292	-0.00123	-2.0641	0.1431	-0.00148 *	1
	Myrsine coriacea	BlEvTrp	-2.0376	0.1250	-0.00090	-1.8753	0.1106	-0.00060 *	1
	Clethra cuneata	BlEvTrp	-2.6686	0.1269	-0.00067	-2.4671	0.1099	-0.00034 *	2
	Miconia aristata	BlEvTrp	-2.2892	0.1433	-0.00115	-1.9709	0.1230	-0.00084 *	1
	Cinchona macrocalyx	BlEvTrp	-2.3650	0.1252	-0.00078	-2.3347	0.1225	-0.00073	1
	Styrax camporum	BlEvTrp	-4.4804	0.1631	-0.00131	-4.5086	0.1658	-0.00137 *	1
	Cinnamomum floccosum	BlEvTrp	-2.1917	0.1531	-0.00124	-1.5127	0.0892	0.00014 *	1
	Axinaea sp	BlEvTrp	-2.2143	0.1362	-0.00102	-2.8795	0.2082	-0.00280	1
	Clusia flaviflora	BlEvTrp	-1.8115	0.0953	-0.00011	-2.0457	0.1151	-0.00050 *	1
	Clusis alata	BlEvTrp	-1.3958	0.0329	0.00102	-1.3958	0.0329	0.00102 *	1
	Persea buchtienii	BlEvTrp	-2.2601	0.1430	-0.00105	-2.0153	0.1206	-0.00058 *	1
	Ocotea spp.	BlEvTrp	-2.6109	0.1536	-0.00122	-2.2858	0.1256	-0.00067 *	1
	Podocarpus oleifolius	BlEvTrp	-0.4915	0.0412	0.00028	-0.0561	0.0054	0.00096 *	1
	Hedyosmum maximum	BlEvTrp	-2.0450	0.1248	-0.00090	-1.8668	0.1059	-0.00043	1
Tropical Rainforest (low altitude)									
San Isidro, Costa Rica							**15-35 ºC**		
	Koanophyllon hylonomum	BlEvTrp	-4.4967	0.2029	-0.00231	-5.1167	0.2507	-0.00318	3
	Pousandra trianae	BlEvTrp	-3.9626	0.1184	-0.00064	-2.5770	0.0130	0.00128	3
	Rinorea hummelii	SEv	-3.8955	0.0779	0.00005	-3.2626	0.0344	0.00074	5
	Carapa guianensis	BlEvTrp	-2.7577	0.1149	-0.00084	-2.5982	0.1056	-0.00073	2
	Anaxagorea crasipetala	BlEvTrp	-3.9297	0.1134	-0.00044	-4.0310	0.1166	-0.00042	3
Atherton, QLD, AUS							**15-35 ºC**		
	Cardwellia sublimis	BlEvTrp	-2.7427	0.1021	-0.00030	-2.4395	0.0735	0.00032	3

Crytocarya mackinnoniana	BlEvTrp	-1.3421	0.0119	0.00105	-0.9970	-0.0129	0.00165	4
Ficus leptoclada	BlEvTrp	-2.2058	0.1237	-0.00091	-2.1171	0.1130	-0.00065	3
Litsea leefeana	BlEvTrp	-2.1555	0.0678	0.00008	-2.0273	0.0523	0.00046	4
Myristica globosa	BlEvTrp	-2.2019	0.0611	0.00028	-2.1753	0.0614	0.00024	3
Polyscia elegans	BlEvTrp	-2.8780	0.1276	-0.00087	-2.8556	0.1217	-0.00069	4
Alphitonia whitei	BlEvTrp	-2.2374	0.0791	-0.00004	-1.7981	0.0415	0.00072	4
Prunus Turneriana	BlEvTrp	-2.9065	0.0945	-0.00035	-2.6470	0.0672	0.00027	4
Daphnandra repandula	BlEvTrp	-2.7954	0.1047	-0.00061	-2.8072	0.1045	-0.00058	5
Syzgium johnsonii	BlEvTrp	-2.4436	0.0639	0.00006	-2.5360	0.0737	-0.00017	4
Alstonia muelleriana	BlEvTrp	-1.5932	0.0722	0.00006	-1.8779	0.0920	-0.00027	4
Argyrodendron trifoliolatum	BlEvTrp	-3.0064	0.0624	0.00055	-2.9480	0.0670	0.00062	3
Ceratopetalum succirubrum	BlEvTrp	-3.0005	0.0783	0.00008	-3.1542	0.0885	-0.00008	4
Doryphora aromatica	BlEvTrp	-2.4071	0.0621	0.00011	-2.4481	0.0694	-0.00010	3
Flindersia sp.	BlEvTrp	-2.5958	0.1269	-0.00089	-2.6457	0.1280	-0.00086	4
Gillbeea adenopetala	BlEvTrp	-2.5083	0.1101	-0.00065	-2.2505	0.0985	-0.00059	2
Cape Tribulation, FNQ, AUS						**20-40 °C**		
Acmena graveolens	BlEvTrp	-2.4074	0.1020	-0.00063	-2.4042	0.0953	-0.00042	2
Argyrodendron peralatum	BlEvTrp	-0.8910	-0.0050	0.00088	-1.1259	0.0079	0.00072	3
Cardwellia sublimis	BlEvTrp	-1.7838	0.0581	-0.00005	-0.7921	-0.0084	0.00102	3
Castanospermum australe	BlEvTrp	-1.1452	-0.0103	0.00117	-1.0438	-0.0034	0.00117	4
Cryptocarya mackinnoniana	BlEvTrp	-1.8409	0.0345	0.00036	-10.8186	0.4955	-0.00551	2
Dysoxylum papuanum	BlEvTrp	-2.7655	0.1335	-0.00106	-4.2070	0.2255	-0.00249	4
Elaeocarpus grandis	BlEvTrp	-0.7934	-0.0105	0.00101	-1.0415	0.0001	0.00093	4
Endiandra leptodendron	BlEvTrp	-1.6457	0.0397	0.00028	-1.4596	0.0245	0.00057	2
Gillbeea whypallana	BlEvTrp	-1.4369	0.0332	0.00035	-1.7981	0.0565	0.00000	4
Myristica globosa ssp. Muelleri	BlEvTrp	-1.5947	0.0275	0.00050	-1.6623	0.0267	0.00059	2
Rockinghamia angustifolia	BlEvTrp	-1.8098	0.0395	0.00018	-2.5668	0.0898	-0.00063	4
Syzygium sayeri	BlEvTrp	-1.1741	0.0178	0.00060	-0.7592	-0.0135	0.00116	3
Paracou, French Guiana						**15-35 °C**		
Carapa procera	BlDcTrp	-2.2663	0.1044	-0.00028	-2.5263	0.1200	-0.00049	4
Eperua falcata	BlEvTrp	-2.2418	0.0919	-0.00056	-2.8552	0.1483	-0.00175	4

Eschweilera coriacea	BlEvTrp	-3.1514	0.1587	-0.00124	-3.0363	0.1514	-0.00113	4
Eschweilera parviflora	BlEvTrp	-0.5766	0.0807	-0.00057	1.9239	-0.1705	0.00378	3
Iryanthera hostmannii	BlEvTrp	-1.1419	0.0891	-0.00042	-0.8226	0.0643	0.00003	1
Lecythis persistens	BlEvTrp	-3.2777	0.1455	-0.00123	-2.8076	0.1030	-0.00034	3
Licania alba	BlEvTrp	-0.9058	0.0153	0.00056	-0.5316	-0.0091	0.00094	2
Oxandra asbeckii	BlEvTrp	-1.7297	-0.0122	0.00141	-1.9276	-0.0522	0.00261	2
Protium opacum	BlEvTrp	-3.2236	0.1447	-0.00134	-3.5757	0.1776	-0.00205	2
Recordoxylon speciosum	BlEvTrp	-3.9505	0.1592	-0.00142	-3.9133	0.1517	-0.00120	3
Sterculia pruriens	BlDcTrp	-3.9517	0.1310	-0.00092	-4.8895	0.2560	-0.00486	2
Symphonia globulifera	BlEvTrp	-4.2184	0.1706	-0.00136	-2.0512	0.0559	0.00034	2
Tabebuia insignis	BlEvTrp	-2.8068	0.1479	-0.00130	-3.3238	0.1856	-0.00195	2
Theobroma subincanum	BlEvTrp	-3.1584	0.1239	-0.00084	-2.7808	0.0896	-0.00013	3
Vismia sessilifolia	BlEvTrp	-4.0248	0.1664	-0.00132	-3.3804	0.1656	-0.00159	4
Bocoa prouacensis	BlEvTrp	-3.9077	0.1868	-0.00164	-2.8754	0.1430	-0.00101	4
Carapa procera	BlDcTrp	-2.9805	0.1209	-0.00063	-3.1880	0.1420	-0.00112	3
Eperua falcata	BlDcTrp	-1.7093	0.0936	-0.00049	-1.9368	0.0922	-0.00011	3
Eschweilera coriacea	BlEvTrp	-2.5358	0.0980	-0.00054	-2.9738	0.1400	-0.00147	3
Eschweilera sagotiana	BlEvTrp	-2.6420	0.0894	-0.00053	-4.6014	0.2645	-0.00419	2
Gustavia hexapetala	BlEvTrp	-4.5294	0.2193	-0.00255	-5.4723	0.3086	-0.00449	1
Iryanthera hostmannii	BlEvTrp	-2.8678	0.0895	-0.00028	-2.6035	0.0630	0.00031	1
Iryanthera sagotiana	BlEvTrp	-3.8810	0.1499	-0.00116	-4.0750	0.1718	-0.00169	2
Lecythis persistens	BlEvTrp	-3.2498	0.1223	-0.00074	-3.6328	0.1461	-0.00110	4
Licania alba	BlEvTrp	-2.8305	0.1124	-0.00070	-3.0112	0.1108	-0.00046	2
Licania heteromorpha	BlEvTrp	-2.8893	0.1162	-0.00096	-2.9081	0.1064	-0.00084	3
Licania membranacea	BlEvTrp	-4.8136	0.1859	-0.00157	-4.8841	0.1901	-0.00163	1
Ormosia coutinhoi	BlEvTrp	-3.2368	0.1420	-0.00109	-3.3433	0.1750	-0.00160	2
Oxandra asbeckii	BlEvTrp	-3.3506	0.1440	-0.00134	-3.7607	0.1811	-0.00212	1
Protium opacum	BlEvTrp	-3.2236	0.1447	-0.00134	-3.5757	0.1776	-0.00205	2
Theobroma subincacum	BlEvTrp	-3.5852	0.1530	-0.00156	-3.8224	0.1728	-0.00195	3
Vouacapoua americana	BlEvTrp	-1.3438	-0.0705	0.00287	2.3581	-0.3872	0.00921	1
Iquitos, Peru						**15-35 °C**		

Pourouma indet	BlEvTrp	-4.2885	0.1036	-0.00054	-3.9050	0.0701	0.00014		1
Luehea indet	BlEvTrp	-2.2342	0.0725	0.00021	-1.4819	0.0066	0.00153		1
Hevea pauciflora	BlEvTrp	-4.1570	0.0984	-0.00037	-2.9795	0.0083	0.00129		1
Swartzia polyphylla	BlEvTrp	-4.4804	0.1631	-0.00131	-4.5086	0.1658	-0.00137		1
Neea divaricata	BlEvTrp	-1.7812	0.0749	-0.00010	-0.7534	-0.0179	0.00184		1
Richeria grandis	BlEvTrp	-2.5559	0.1126	-0.00095	-2.5593	0.1107	-0.00088		1
Hymenaea courbaril	BlEvTrp	-3.1474	0.1082	-0.00033	-2.8511	0.0840	0.00013		1
Dipteryx micrantha	BlEvTrp	-1.4854	0.0666	-0.00014	-1.2551	0.0434	0.00037		1
Pouteria subrotata	BlEvTrp	-4.8248	0.1329	-0.00085	-4.2634	0.0988	-0.00035	*	1
Licania arachnoidea	BlEvTrp	-3.2732	0.1239	-0.00060	-2.4037	0.0519	0.00081		1
Guatteria schomburgkiana	BlEvTrp	-3.2384	0.1840	-0.00183	-3.2228	0.1820	-0.00177		1
Minquartia guianensis	BlEvTrp	-1.4949	0.0511	0.00041	-0.8485	-0.0069	0.00161		1
Licaria canella	BlEvTrp	-2.0179	0.0877	-0.00030	-1.2761	0.0256	0.00093		1
Hevea guianensis	BlEvTrp	-3.2384	0.1840	-0.00183	-3.2228	0.1820	-0.00177		1
Cathedra acuminata	BlEvTrp	-5.5706	0.1268	-0.00097	-7.1624	0.2568	-0.00357		1
Taralea oppositifolia	BlEvTrp	-3.3512	0.1422	-0.00084	-3.2085	0.1317	-0.00067		1